JACS
JOURNAL OF THE AMERICAN CHEMICAL SOCIETY
Article
pubs.acs.org/JACS

Heterobimetallic Porphyrin Complexes Displaying Triple Dynamics: Coupled Metal Motions Controlled by Constitutional Evolution

Stéphane Le Gac,*[,†] Luca Fusaro,[‡] Thierry Roisnel,[†] and Bernard Boitrel*[,†]

[†]UMR CNRS 6226, Institut des Sciences Chimiques de Rennes, Université de Rennes 1, 263 Avenue du Général Leclerc, 35042 Rennes Cedex, France

[‡]Laboratoire de RMN Haute Résolution, Université Libre de Bruxelles, CP 160/08, 50 Avenue F.-D. Roosevelt, B-1050, Bruxelles, Belgium

Supporting Information

ABSTRACT: A bis-strap porphyrin ligand (**1**), with an overhanging carboxylic acid group on each side of the macrocycle, has been investigated toward the formation of dynamic libraries of bimetallic complexes with Hg(II), Cd(II), and Pb(II). Highly heteroselective metalation processes occurred in the presence of Pb(II), with Hg(II) or Cd(II) bound *out-of-plane* to the N-core and "PbOAc" bound to a carboxylate group of a strap on the opposite side. The resulting complexes, $\mathbf{1}_{Hg}$**·PbOAc** and $\mathbf{1}_{Cd}$**·PbOAc**, display three levels of dynamics. The first is *strap-level (interactional dynamics)*, where the PbOAc moiety swings between the left and right side of the strap owing to a second sphere of coordination with lateral amide functions. The second is *ligand-level (motional dynamics)*, where $\mathbf{1}_{Hg}$**·PbOAc** and $\mathbf{1}_{Cd}$**·PbOAc** exist as two degenerate states in equilibrium controlled by a chemical effector (AcO^-). The process corresponds to a double translocation of the metal ions according to an intramolecular migration of Hg(II) or Cd(II) through the N-core, oscillating between the two equivalent overhanging carbonyl groups, coupled to an intermolecular pathway for PbOAc exchanging between the two equivalent overhanging carboxylate groups (N-core^{up} ⇆ N-core^{down} coupled to strap^{down} ⇆ strap^{up}, i.e., coupled motion #1 in the abstract graphic). The third is *library-level (constitutional dynamics)*, where a dynamic constitutional evolution of the system was achieved by the successive addition of two chemical effectors (DMAP and then AcO^-). It allowed shifting equilibrium forward and backward between $\mathbf{1}_{Hg}$**·PbOAc** and the corresponding homobimetallic complexes $\mathbf{1Hg_2}$**·DMAP** and $\mathbf{1}_{Pb}$**·PbOAc**. The latter displays a different ligand-level dynamics, in the form of an intraligand coupled migration of the Pb(II) ions (N-core^{up} ⇆ strap^{up} coupled to strap^{down} ⇆ N-core^{down}, i.e., coupled motion #2 in the abstract graphic). In addition, the neutral "bridged" complexes **1HgPb** and **1CdPb**, with the metal ions on opposite sides both bound to the N-core and to a carboxylate of a strap, were structurally characterized. These results establish an unprecedented approach in supramolecular coordination chemistry, by considering the reversible interaction of a metal ion with the porphyrin N-core as a new source of self-organization processes. This work should provide new inspirations for the design of innovative adaptative materials and devices.

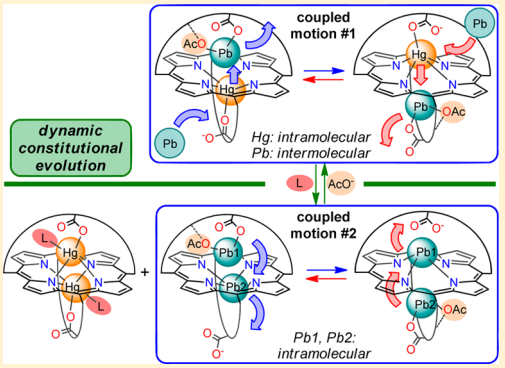

INTRODUCTION

Adaptative chemistry refers to dynamic systems (covalent or noncovalent assemblies) able to undergo a modification of their composition as a consequence of a modification of their environment, resulting in new properties or functions (sensing, catalysis, transport, etc.).[1] It is rooted in constitutional dynamic chemistry,[2] a branch of supramolecular chemistry focusing on self-organization processes in dynamic libraries (ensembles of molecules or assemblies in equilibrium, made of reversibly connected units). Formed under thermodynamic control, these libraries are prone to undergo amplification processes in response to an external trigger, leading to the self-emergence of structures that are best adapted to the new sets of physical or chemical parameters, through reorganization of their constitutive units. Adaptative molecular systems are attractive to design ever complex (smart) materials and devices.[3]

Metalloporphyrins have been widely used as subcomponents in the construction of supramolecular edifices, with vast applications in the fields of molecular recognition, artificial photosynthesis, catalysis, materials, and others. Supramolecular coordination chemistry using axial ligation to the porphyrin metal center is among the most common strategies allowing the engineering of complex structures via self-organization processes.[4] In many cases, the use of a template agent is used to select a particular arrangement among oligomeric or undesired assemblies, but it is worthwhile to note that few metalloporphyrin-based supramolecular systems have been analyzed in terms of dynamic constitutional libraries. The group of Sanders has investigated dynamic libraries of metalloporphyrins based on metal−phosphine ligation[5] and

Received: February 24, 2014
Published: April 21, 2014

   dx.doi.org/10.1021/ja501926f | J. Am. Chem. Soc. 2014, 136, 6698−6715

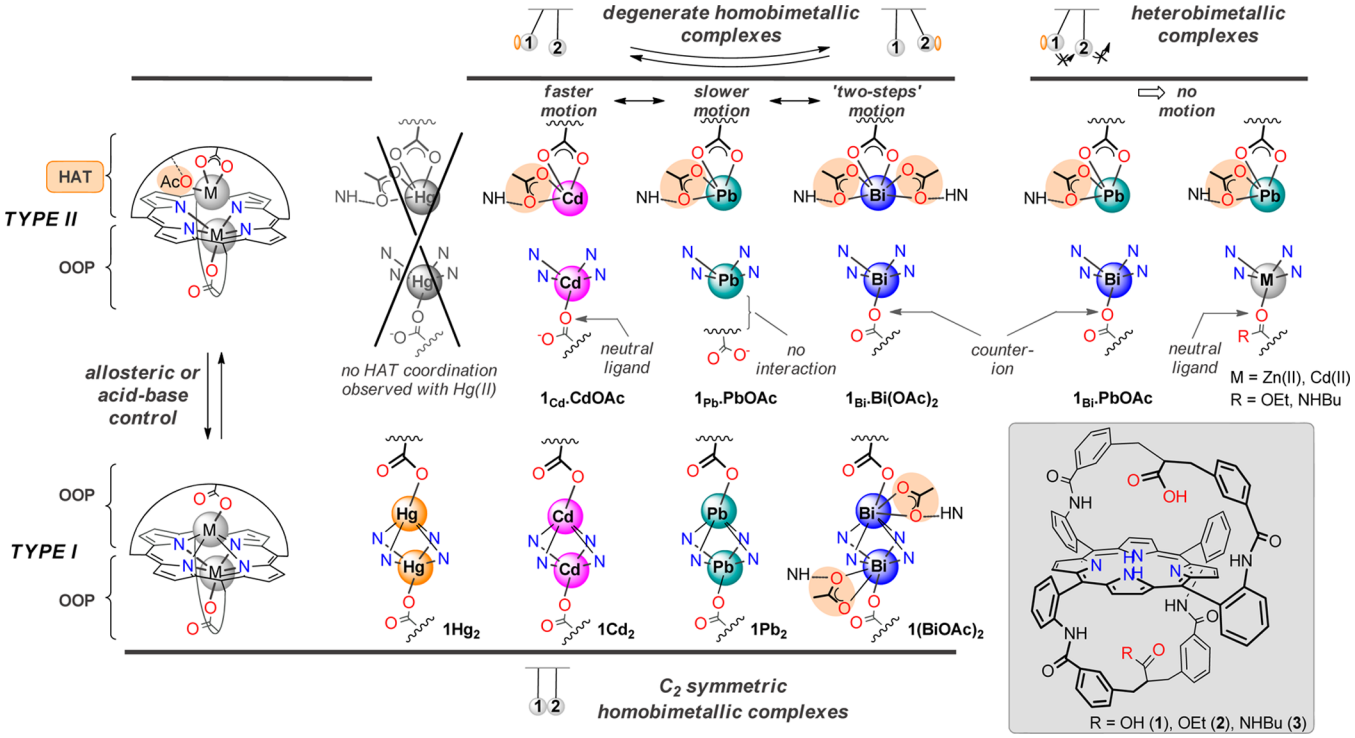

Figure 1. Overview of the various bimetallic complexes previously obtained from overhanging carboxylic acid porphyrins **1**−**3** (structures in inset) and their dynamic behavior (HAT = hanging-atop; OOP = out-of-plane; exogenous acetates are highlighted by a tan oval).

has shown the selection of molecular receptors in response to the addition of guest molecules. More recently, a dynamic library approach was used by Handerson et al. for the templated formation of zinc porphyrin nanorings. The ratio of nanorings of different sizes (e.g., rings made of 16 vs 24 porphyrins) indeed depends on the amount of a template agent, suggesting the formation of dynamic libraries of self-assembled complexes prior to covalent trapping.[6,7]

In general, the supramolecular coordination chemistry of metalloporphyrins is dominated by the use of a small metal ion [Zn(II), Mg(II), Al(III), Ru(II), Rh(III), etc.] that fits into the N-core of the macrocycle (*in-plane* coordination), with high stability.[4] This is obviously desirable for their integration into functional devices or materials for which robustness is often a prerequisite. Conversely, it came to us that the use of kinetically labile metal porphyrin complexes could furnish an additional tool in the formation of adaptative systems, by considering the reversible interaction of a metal ion with the N-core as a new source of self-organization processes. To the best of our knowledge, adaptative systems based on metalloporphyrins exchanging their N-core bound metal ion(s) (through reversible transmetalations for instance) in response to an external stimulus have not been described so far.[8] To build up a proof of concept, we considered the use of a ditopic porphyrin chelate as a platform for the binding of two metal ions and of different metal ions as subcomponents that can self-organize by reversible binding to the platform. By doing so, several combinations of homo and heterobimetallic species would be virtually accessible, thus defining a dynamic library of metalloporphyrins. This strategy lies on recent results from our group obtained with bis-strap overhanging carboxylic acid(s) porphyrins.[9,10] We have indeed shown that two types of bimetallic complexes were accessible with such ditopic chelates (Figure 1). On the one hand, "bridged" C_2-symmetric homobimetallic species with the metal ions on opposite sides both bound to the porphyrin N-core and to a carboxylate of a strap (type I, lower part in Figure 1) were observed with the C_2-symmetric chelate **1** and Hg(II),[9b] Cd(II),[9f] Pb(II),[9d] and Bi(III)[9d] ions [$\mathbf{1Hg_2}$, $\mathbf{1Cd_2}$, $\mathbf{1Pb_2}$, and $\mathbf{1(BiOAc)_2}$].[11] On the other hand, heterobimetallic species were obtained with a metal ion bound to the N-core and a second metal ion bound on the opposite side to a carboxylate of a strap, in a so-called *hanging-atop* (HAT) coordination mode (type II, upper part in Figure 1).[12] They were observed with **1**, Bi(III), and Pb(II) ($\mathbf{1_{Bi}}$·**PbOAc**)[9d,13] and with **2** or **3**, Zn(II) or Cd(II), and Pb(II).[9e] In these complexes, the PbOAc moiety is stabilized by a crucial second sphere of coordination (H-bond with the amide group(s) of a strap). Interestingly, type I homobimetallic complexes were converted to type II by addition of AcO^- in the case of Pb(II) and Cd(II) ($\mathbf{1_{Pb}}$·**PbOAc** and $\mathbf{1_{Cd}}$·**CdOAc**) and by addition of a base with Bi(III) [$\mathbf{1_{Bi}}$·**Bi(OAc)$_2$**] (upper middle part, Figure 1). The last three complexes are present as two degenerate states in equilibrium, according to a unique intraligand coupled motion of the metal ions, formally a double translocation process under allosteric control ($strap^{up} \leftrightarrows$ N-$core^{up}$ coupled to N-$core^{down} \leftrightarrows strap^{down}$).[14,15] This coupled migration resembles the motion of spheres in a Newton's cradle device, since the metal ions remain on their respective side of the macrocycle while exchanging between HAT and *out-of-plane* (OOP) coordination modes (compartmentalized motion).[9d,f,i] Such a motional dynamics of the metal ions is not observed with type II heterobimetallic complexes. Thus, whereas intramolecular transmetalation readily occurs in the coupled motion of the metal ions (type II homobimetallic complexes), intermolecular transmetalations are also effective: it allowed the successive formation of three different Pb(II)/Bi(III) bimetallic complexes via selective metal exchange reactions [$\mathbf{1_{Pb}}$·**PbOAc** → $\mathbf{1_{Bi}}$·**PbOAc** → $\mathbf{1_{Bi}}$·**Bi(OAc)$_2$**], which

dx.doi.org/10.1021/ja501926f | J. Am. Chem. Soc. 2014, 136, 6698−6715

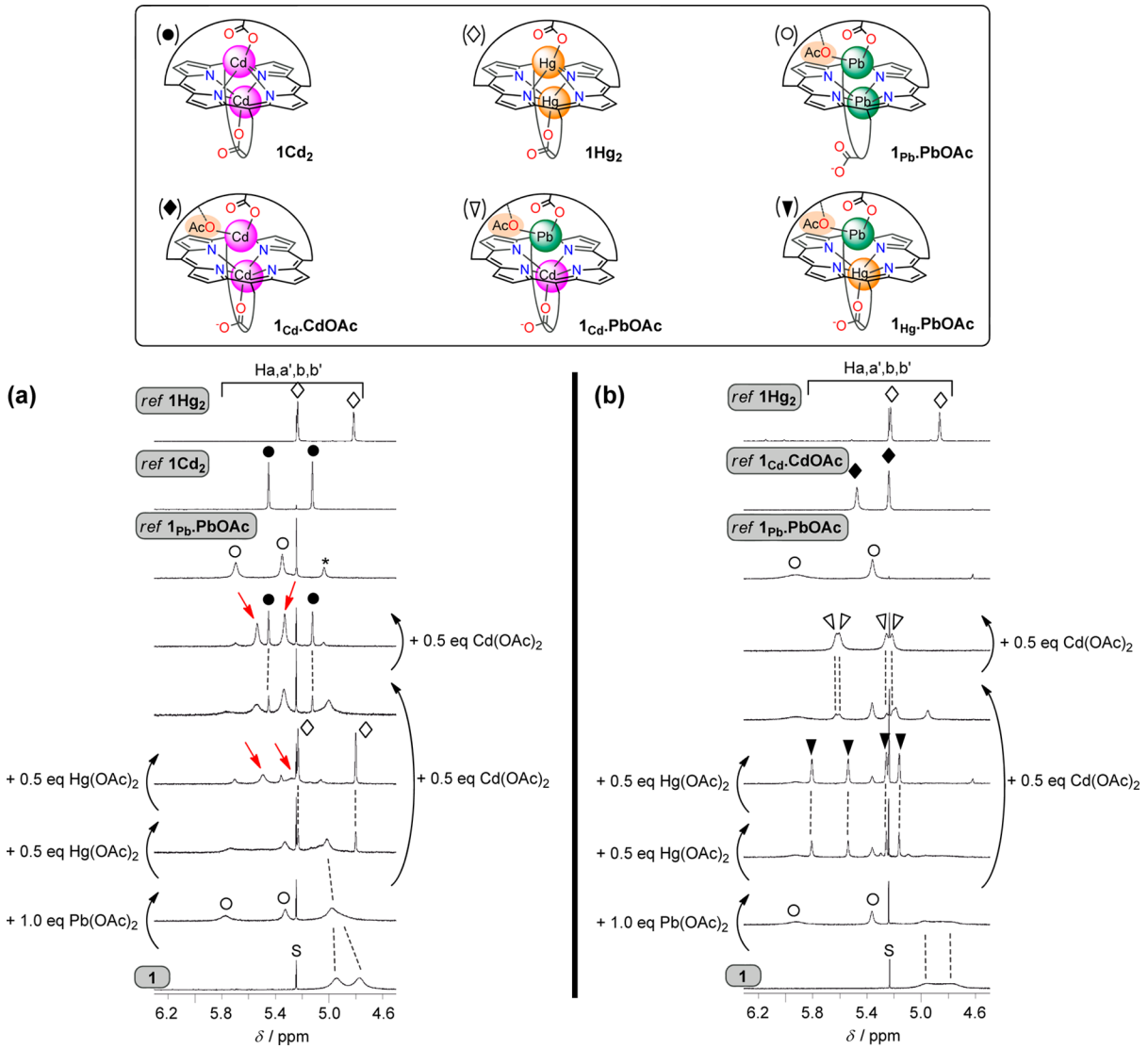

Figure 2. ^{1}H NMR study (298 K, 500 MHz, $CDCl_3/CD_3OD$ 9:1, partial spectra) related to the formation of Hg(II)/Pb(II) and Cd(II)/Pb(II) heterobimetallic complexes with ligand **1**, in the absence (a) and with 15 equiv of DIPEA (b). Top: reference spectra of the homobimetallic complexes under the same experimental conditions. For proton labeling, see Scheme 1. Red arrows indicate ill-resolved signals that may correspond to heterobimetallic complexes. S = trace of residual solvent; * = impurity.

is a means to control the motional dynamics of the metal ions (fast motion → no motion → slow motion).[9c,d] It is worth mentioning that the lability of these complexes relies on (i) the overhanging COO^- groups, which help insertion and exchange of the metal ions (in general, instantaneous processes at room temperature),[16] and (ii) the size, medium to large, of these heavy metals, responsible for important deviations from the mean plane (OOP coordination).[17] On these bases, we have investigated the formation of heterobimetallic complexes with the C_2-symmetric ligand **1** and divalent metal ions as Hg(II), Cd(II), and Pb(II), aiming at new kinds of dynamic libraries of metalloporphyrins that could feature adaptative behaviors.

RESULTS

1. Selectivity Study for the Formation of Heterobimetallic Species with Pb(II), Hg(II), and Cd(II). In a first set of experiments, we have investigated the formation of Hg(II)/Cd(II) heterobimetallic complexes with ligand **1**. For that purpose, ^{1}H NMR titration experiments of **1** with $Hg(OAc)_2$ and $Cd(OAc)_2$ solutions have been conducted in a 9:1 $CDCl_3/CD_3OD$ mixture, in the absence and with excess of diisopropylethylamine (DIPEA) [see the Supporting Information (SI)]. For all investigated conditions, equilibrium was reached instantaneously, and the ratios of the different species were independent of the order of introduction of the metal salts, indicating thermodynamic control. In the presence of DIPEA, addition of 1 equiv of $Hg(OAc)_2$ and 1 equiv of $Cd(OAc)_2$ to **1** led to the formation of $\mathbf{1Hg_2}$, together with one or several undefined species characterized by broad NMR patterns, different from those of the known monometallic and homobimetallic species of **1**.[18] The composition of the mixture was significantly affected neither at low temperature (down to 223 K) nor by the addition of an excess of both metal salts, whereas the addition of an excess of only one of the metal salts led to the formation of the corresponding homobimetallic complex as a major product ($\mathbf{1Cd_2}$ or $\mathbf{1Hg_2}$). In the absence of base, the addition of 1 equiv of both $Hg(OAc)_2$ and $Cd(OAc)_2$ to **1** led to the formation of $\mathbf{1Hg_2}$, $\mathbf{1Cd_2}$, and a new species with sharp signals, in a statistical 1:1:1 ratio. The newly formed

dx.doi.org/10.1021/ja501926f | J. Am. Chem. Soc. 2014, 136, 6698−6715

Scheme 1. Formation of Hg(II)/Pb(II) and Cd(II)/Pb(II) Heterobimetallic Complexes[a]

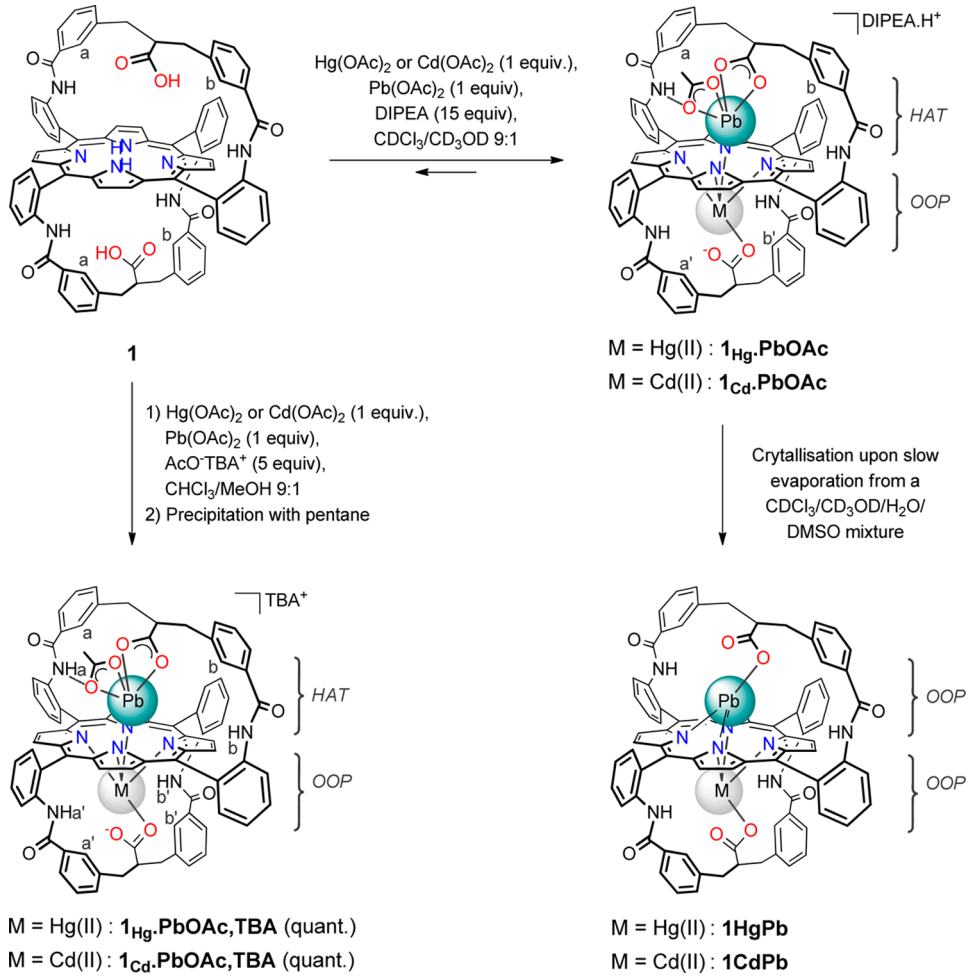

[a](Top) Selective formation of the heterobimetallic complexes $\mathbf{1}_{Hg}$·**PbOAc** and $\mathbf{1}_{Cd}$·**PbOAc** (DIPEA·H$^+$ salts) as deduced from ^{1}H NMR titration studies. (Left) Synthesis of analytical samples of the heterobimetallic complexes $\mathbf{1}_{Hg}$·**PbOAc,TBA** and $\mathbf{1}_{Cd}$·**PbOAc,TBA** (TBA$^+$ salts). (Right) Formation of the neutral heterobimetallic complexes **1HgPb** and **1CdPb** (single crystals suitable for XRD analysis).

species displays a dissymmetric pattern, indicating that both sides of the ligand are different and may likely be assigned to a heterobimetallic Hg(II)/Cd(II) complex (**1HgCd**, SI) although strong overlapping of the signals hampered further structural investigations. The addition of a slight excess of both metal salts (2 equiv) led quantitatively to $\mathbf{1Hg_2}$. These results show that mixtures of homobimetallic and a fortiori heterobimetallic complexes can be obtained under thermodynamic conditions, with possible evolution of their constitutions, which supports the formation of dynamic libraries of metalloporphyrins.

In the same solvent, Pb(II) was then combined with Hg(II) or Cd(II) and **1** (Figure 2). Again, equilibrium was reached instantaneously, and the ratios of the different species were independent of the order of introduction of the metal salts. Without base, the metalation of **1** with $Hg(OAc)_2$/$Pb(OAc)_2$ or $Cd(OAc)_2$/$Pb(OAc)_2$ led to mixtures of bimetallic complexes in all investigated M1/M2/**1** ratios (Figure 2a). The homobimetallic complexes $\mathbf{1Hg_2}$ or $\mathbf{1Cd_2}$ were clearly observed at a 1:1:1 M1/M2/**1** ratio, together with unidentified species displaying broad NMR patterns (see red arrows). Heterobimetallic complexes may be formed, but further structural investigations were hampered by the low resolution of their NMR patterns with strong overlapping of most of the signals even at low temperature (223 K). In contrast, with 15 equiv of DIPEA in the media, addition of 1 equiv of $Pb(OAc)_2$ to **1** followed by 1 equiv of $Hg(OAc)_2$ or $Cd(OAc)_2$ led, in both cases, to the selective and virtually quantitative formation of a new species (Figure 2b, filled and hollow triangles).[19] The four aromatic protons of the straps, Ha, Hb, Ha′, and Hb′ (see labeling in Scheme 1), resonate at 5.81, 5.54, 5.26, and 5.16 ppm for Pb/Hg and at 5.62, 5.60, 5.27, and 5.21 ppm for Pb/Cd. This evidenced the formation of dissymmetric species with a different metal ion on each side of the porphyrin macrocycle. The broad and slightly high-field-shifted signal of the acetate anions indicates their participation in the complexes, in a fast exchange regime at room temperature. Low-temperature NMR measurements such as 2D ROESY experiments revealed a single bound acetate (slow exchange regime at 223 K), observed as a singlet at +0.18 and +0.28 ppm for Pb/Hg and Pb/Cd, respectively (vide infra and see the SI). These chemical shifts agree with the presence of a hanging-atop metal ion. More particularly, they are consistent with a PbOAc moiety hung over the N-core, as deduced from comparison with the chemical shifts of the bound acetate in the known complexes $\mathbf{1}_{Pb}$·**PbOAc** and $\mathbf{1}_{Cd}$·**CdOAc** formed in the same experimental conditions.[20] We therefore propose the formation of the heterobimetallic complexes $\mathbf{1}_{Hg}$·**PbOAc** and $\mathbf{1}_{Cd}$·**PbOAc** (Scheme 1, top), with Hg(II) and Cd(II) bound to the N-

dx.doi.org/10.1021/ja501926f | J. Am. Chem. Soc. 2014, 136, 6698−6715

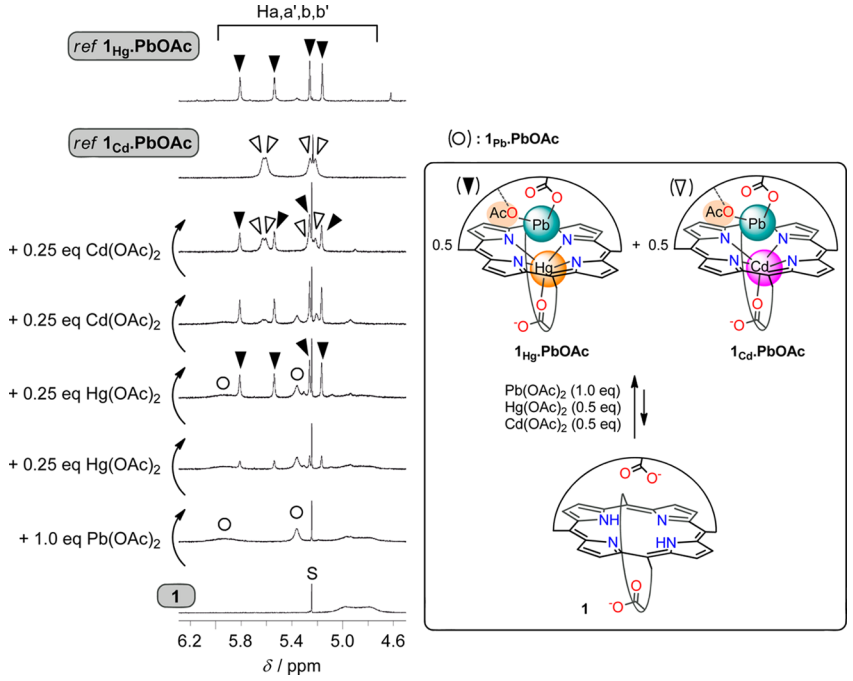

Figure 3. Partial ^{1}H NMR spectra (298 K, 500 MHz, $CDCl_3/CD_3OD$ 9:1 with 15 equiv of DIPEA) of **1** before and upon the successive addition of 1 equiv of $Pb(OAc)_2$, 0.5 equiv of $Hg(OAc)_2$, and 0.5 equiv of $Cd(OAc)_2$ (from bottom to top). (Top) Reference spectra of the heterobimetallic complexes under the same experimental conditions. For proton labeling, see Scheme 1. S = trace of residual solvent.

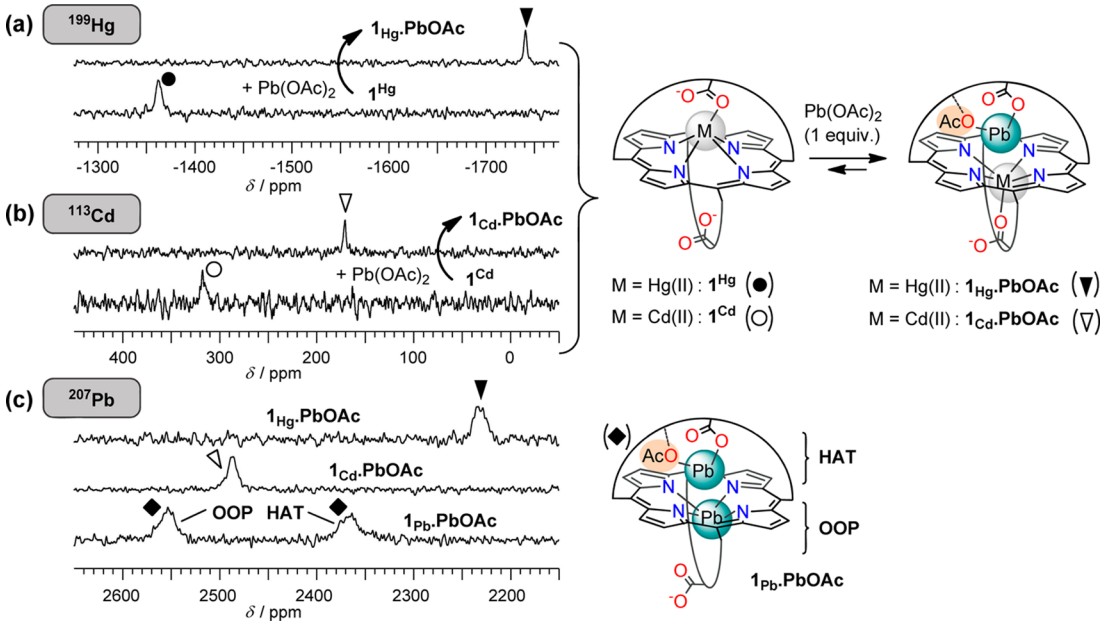

Figure 4. ^{199}Hg, ^{113}Cd, and ^{207}Pb heteronuclear NMR monitoring ($CDCl_3/CD_3OD$ 9:1, 9.4 T, 298 K, with 7.5 equiv of DIPEA) of the formation of $\mathbf{1_{Hg}}$**·PbOAc** and $\mathbf{1_{Cd}}$**·PbOAc:** (a) ^{199}Hg NMR spectra (71.6 MHz) of $\mathbf{1}^{Hg}$ before and after addition of 1 equiv of $Pb(OAc)_2$, leading to $\mathbf{1_{Hg}}$**·PbOAc**. (b) ^{113}Cd NMR spectra (88.7 MHz) of $\mathbf{1}^{Cd}$ before[9f] and after addition of 1 equiv of $Pb(OAc)_2$, leading to $\mathbf{1_{Cd}}$**·PbOAc**. (c) ^{207}Pb NMR spectra (83.6 MHz) of $\mathbf{1_{Hg}}$**·PbOAc**, $\mathbf{1_{Cd}}$**·PbOAc**, and $\mathbf{1_{Pb}}$**·PbOAc** (the latter homobimetallic complex formed upon addition of 2 equiv of $Pb(OAc)_2$ to **1**). HAT and OOP stand for hanging-atop and out-of-plane, respectively.

core and a PbOAc moiety bound to the overhanging carboxylate on the opposite side. HRMS analysis confirmed the incorporation of "Hg(/Cd)PbOAc" in **1** (see the Experimental Section).

Both complexes tolerate an excess of $Pb(OAc)_2$ (up to ca. 2 equiv), which is due to the higher affinity of the smaller cations Hg(II) and Cd(II) for the N-core. The complex $\mathbf{1_{Cd}}$**·PbOAc** also tolerates an excess of $Cd(OAc)_2$ (up to ca. 2 equiv), showing a higher affinity of a PbOAc moiety for the HAT binding site vs a CdOAc one.[21] In contrast, the further addition of 1 equiv of $Hg(OAc)_2$ to $\mathbf{1_{Hg}}$**·PbOAc** led to the almost quantitative formation of $\mathbf{1Hg_2}$. Thus, similarly to Hg(II)/Cd(II), dynamic libraries of bimetallic complexes are generated with Cd(II)/Pb(II) and Hg(II)/Pb(II), with a strong amplification of the heterobimetallic complexes $\mathbf{1_{Hg}}$**·PbOAc** and $\mathbf{1_{Cd}}$**·PbOAc** in the presence of DIPEA. The deprotonation

dx.doi.org/10.1021/ja501926f | J. Am. Chem. Soc. 2014, 136, 6698−6715

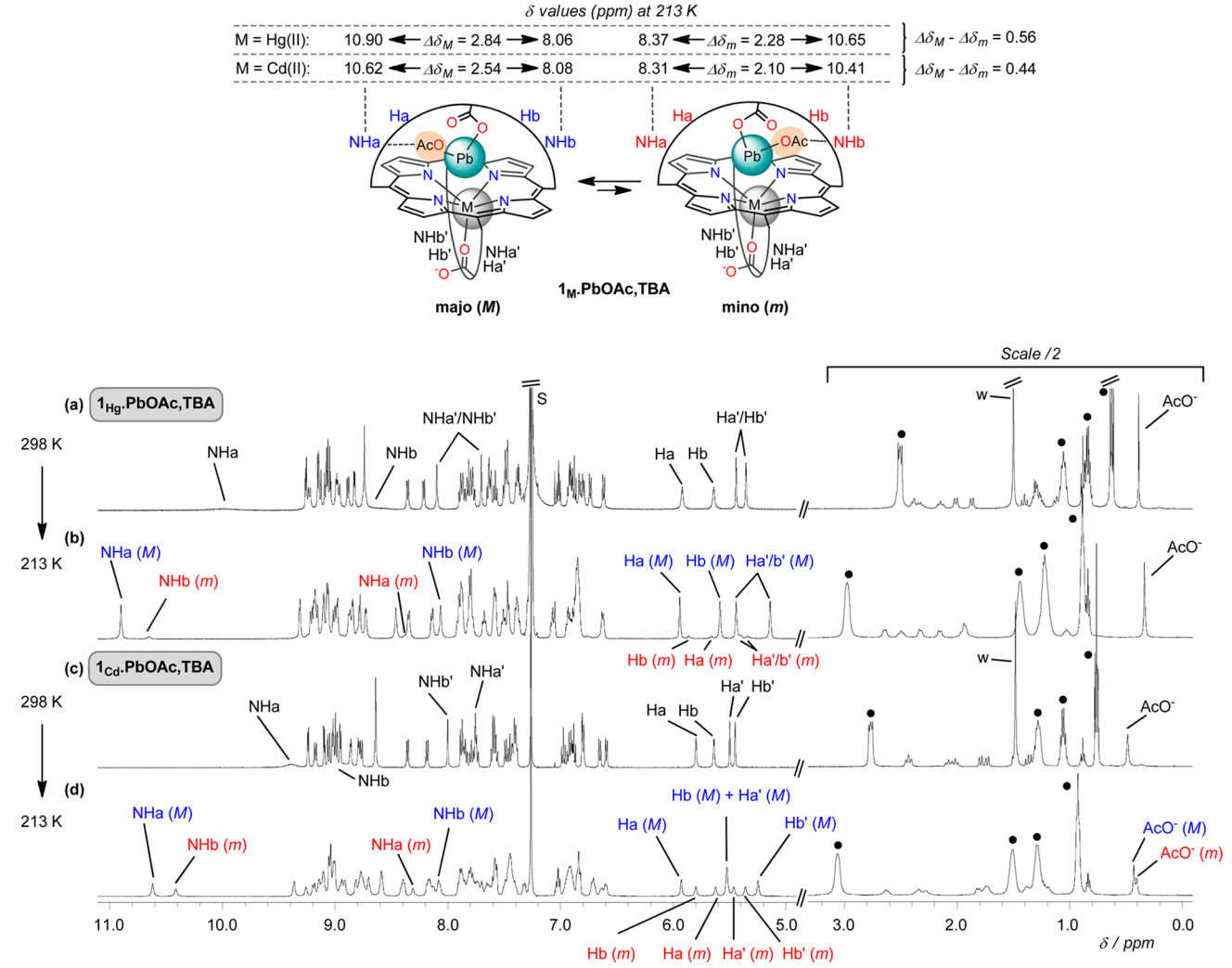

Figure 5. ^{1}H NMR spectra (500 MHz, $CDCl_3$) of analytical samples of $\mathbf{1}_{Hg}$**·PbOAc,TBA** at 298 K (a) and 213 K (b) and $\mathbf{1}_{Cd}$**·PbOAc,TBA** at 298 K (c) and 213 K (d). "●" indicates TBA^+, S = solvent, W = water; for proton labeling, see Scheme 1

state of the overhanging COO^- group that binds apically the N-core-bound Hg(II) and Cd(II) cation (N_4O coordination sphere, Scheme 1) is a key parameter. As observed with related complexes,[9e,f] the carbonyl−metal interaction is responsible for an important out-of-plane displacement of the cations (up to ca. 0.9 Å) along with a dome-shaped conformation of the porphyrin. This increases the complementarity of the HAT Pb(II) cation with the strap binding site, on the opposite side. As the carbonyl−metal interaction is stronger with a COO^- than with a COOH group, amplification of $\mathbf{1}_{Hg}$**·PbOAc** and $\mathbf{1}_{Cd}$**·PbOAc** occurs under basic conditions.[22] Such a high degree of selectivity is best exemplified by the following experiment, mixing the three metal salts together. To a solution of **1** in a 9:1 $CDCl_3/CD_3OD$ mixture in the presence of DIPEA were successively added 1 equiv of $Pb(OAc)_2$, 0.5 equiv of $Hg(OAc)_2$, and 0.5 equiv of $Cd(OAc)_2$. Equilibria were reached instantaneously and the corresponding NMR spectrum showed the formation of $\mathbf{1}_{Hg}$**·PbOAc** and $\mathbf{1}_{Cd}$**·PbOAc** (1:1 ratio) as the only observable species (Figure 3). These two heterobimetallic complexes coexist in solution and are selectively obtained out of at least eight possible species (two monometallic complexes,[23] three homobimetallic complexes, and three heterobimetallic complexes).

Heteronuclear NMR experiments were also used to monitor the formation of these Pb(II) heterobimetallic complexes, owing to the natural abundance of the spin-$^1/_2$ ^{199}Hg, ^{113}Cd, and ^{207}Pb nuclei.[24−26] First, the monometallic complexes $\mathbf{1}^{Hg}$ and $\mathbf{1}^{Cd}$ (simplified structures in Figure 4) were formed by addition of 1 equiv of $Hg(OAc)_2$ and $Cd(OAc)_2$, respectively, to **1** in the presence of DIPEA (9:1 $CDCl_3/CD_3OD$).[9b,f] The further addition of 1 equiv of $Pb(OAc)_2$ led to $\mathbf{1}_{Hg}$**·PbOAc** and $\mathbf{1}_{Cd}$**·PbOAc**. At 298 K, ^{199}Hg and ^{113}Cd NMR spectra of these four metal complexes are characterized by a single resonance, and in both cases, an important high-field shift with a sharpening of the signals is observed upon the formation of the bimetallic complexes (Figure 4a,b, $\Delta\delta^{199}_{Hg} = -379$ ppm, $\Delta\delta^{113}_{Cd} = -147$ ppm). These heteronuclear NMR measurements thus appear very sensitive, the close proximity of the HAT Pb(II) being strongly experienced by the N-core-bound cation. Although the N_4O coordination spheres of Hg(II) and Cd(II) should remain roughly the same in the mono- and bimetallic complexes (see Figure 4), a higher out-of-plane displacement is expected in the heterobimetallic complexes due to electrostatic repulsion with the HAT Pb(II) cation.[9d,e] At 298 K, the ^{207}Pb spectra of $\mathbf{1}_{Hg}$**·PbOAc** and $\mathbf{1}_{Cd}$**·PbOAc** revealed a single resonance at respectively 2214 and 2466 ppm (Figure 4c). For comparison, the ^{207}Pb spectrum of the related

dx.doi.org/10.1021/ja501926f | J. Am. Chem. Soc. 2014, 136, 6698−6715

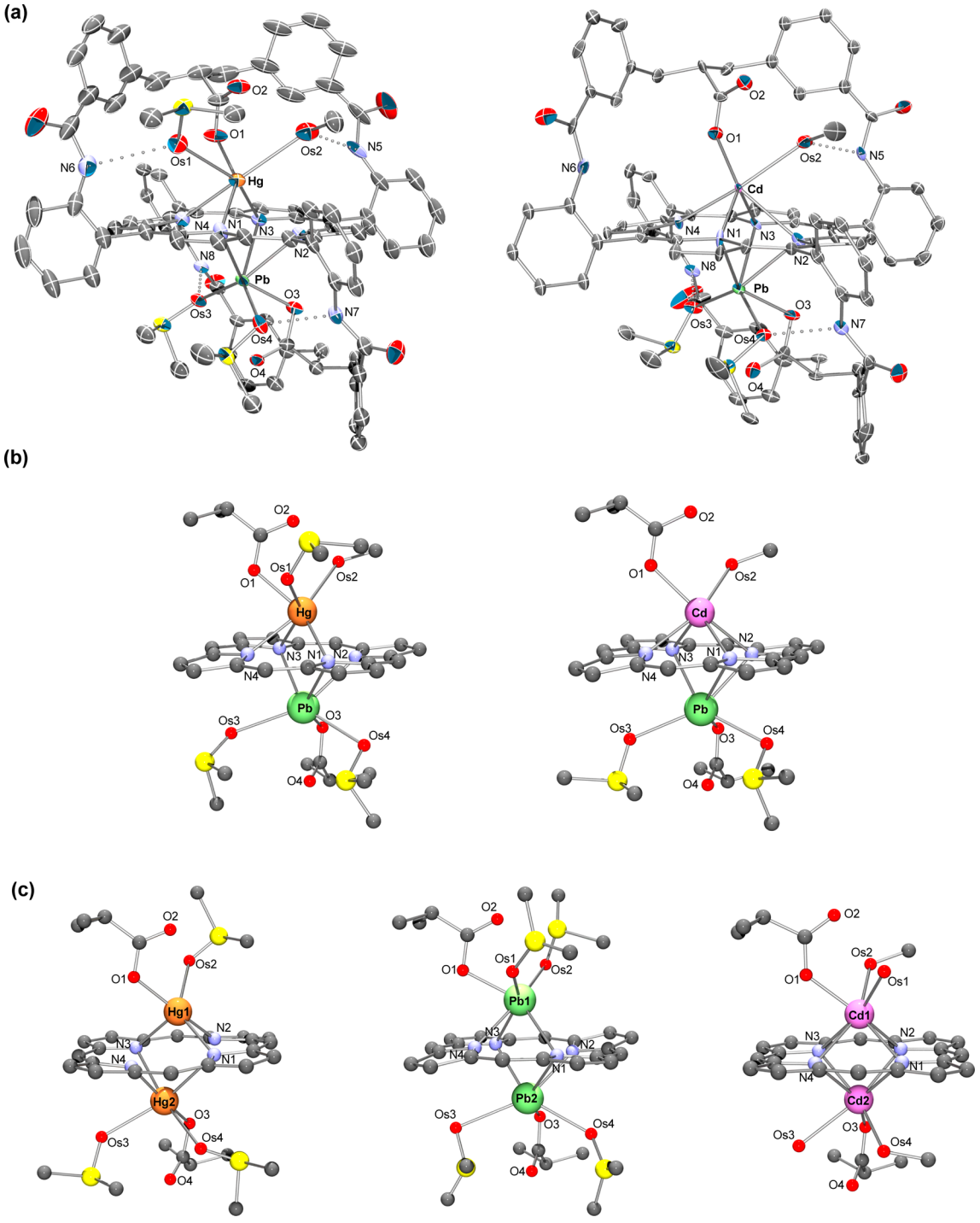

Figure 6. (a) Crystal structures of the neutral heterobimetallic complexes **1HgPb** (left) and **1CdPb** (right) (Ortep views at 30% level of probability; H atoms and solvents of crystallization removed for clarity). (b) Ball and stick views of the coordination sphere of the lead, cadmium, and mercury atoms in the crystal structures of **1HgPb** (left) and **1CdPb** (right) and (c) comparison with that of the same elements in the related homobimetallic complexes $\mathbf{1Hg_2}$,[9b] $\mathbf{1Pb_2}$,[9a] and $\mathbf{1Cd_2}$.[9f] For $\mathbf{1Pb_2}$ and $\mathbf{1Hg_2}$, Os1−Os4 are oxygen atoms of DMSO molecules. For $\mathbf{1Cd_2}$, Os2 and Os4 are methanol molecules, Os1 and Os3 being water molecules.

complex $\mathbf{1_{Pb}}$**·PbOAc**, recorded at 298 K, displays two signals in a 1:1 ratio at 2553 and 2363 ppm that were assigned to the OOP Pb(II) and HAT Pb(II), respectively (Figure 4c).[27] Similarly to the N-core-bound metal ions, the ^{207}Pb nucleus is also quite sensitive to the presence of a second metal ion.

2. Preparation of Analytical Samples of the Heterobimetallic Complexes $\mathbf{1_{Hg}}$·PbOAc and $\mathbf{1_{Cd}}$·PbOAc. The synthesis of analytical samples of complexes $\mathbf{1_{Hg}}$**·PbOAc** and $\mathbf{1_{Cd}}$**·PbOAc** was then undertaken. After several attempts, we observed that the purification of the complexes was easier in the form of their tetrabutylammonium salt. Thus, they have been synthesized using 1 equiv of $Hg(OAc)_2$ or $Cd(OAc)_2$, 1 equiv of $Pb(OAc)_2$, and 5 equiv of AcO^-TBA^+ instead of DIPEA, in a 9:1 $CHCl_3/CH_3OH$ mixture. The metalations proceeded instantaneously at room temperature. Removal of the excess of AcO^-TBA^+ by precipitation in a chloroform/pentane

dx.doi.org/10.1021/ja501926f | J. Am. Chem. Soc. 2014, 136, 6698−6715

Table 1. Selected Distances (Å) and Angles (deg) in the X-ray Crystal Structures of $1Hg_2$,[9b] 1HgPb, $1Pb_2$,[9a] 1CdPb, and $1Cd_2$[9f]

	$1Hg_2$[b]	1HgPb (M2 = Pb)	$1Pb_2$[a]	1CdPb (M2 = Pb)	$1Cd_2$
M2−24MP	1.733	1.856	1.795	1.862	1.510
M1−24MP	1.408	1.549		1.445	1.441
M1−M2	3.258	3.411	3.598	3.309	2.952
(PyrN2−5MP,24MP)[c]	7.84	6.23	11.04	4.12	1.760
(PyrN4−5MP,24MP)[c]	8.34	8.45		10.20	2.450
M1−N1	2.480	2.440		2.391	2.454
M1−N2	2.165	2.757		2.553	2.473
M1−N3	2.533	2.661		2.533	2.515
M1−N4	2.871	2.439		2.377	2.499
M2−N1	2.830	2.833	2.787	2.856	2.532
M2−N2	3.205	2.610	2.480	2.630	2.537
M2−N3	2.673	2.701	2.648	2.693	2.462
M2−N4	2.133	2.916	2.995	2.915	2.502
M1−O1	2.100	2.282		2.304	2.242
M1−O2	3.401	3.135		3.377	3.450
M1−Os1		2.697			2.351
M1−Os2	2.821	2.894		2.609	2.402
M2−O3	2.070	2.278	2.322	2.258	2.224
M2−O4	3.106	2.825	2.975	2.825	3.326
M2−Os3	2.618	2.707	2.651	2.685	2.584
M2−Os4	2.738	2.805	2.832	2.595	2.290

[a]Complex $1Pb_2$ crystallized in the monoclinic space group $C2/c$. Therefore, the two sides of the complex are identical (i.e., Pb1 = Pb2). [b]The distances are those of one of the two isomers present in the crystal lattice. [c]Angle between the mean plane of the pyrrole ring including N2 or N4 atom and the 24-atom porphyrin mean plane.

mixture led to $\mathbf{1}_{Hg}$·**PbOAc,TBA** and $\mathbf{1}_{Cd}$·**PbOAc,TBA** in quantitative yields (Scheme 1, left). HRMS analysis confirmed the incorporation of "Hg(/Cd)PbOAc" in **1** (see the Experimental Section). Their ^{1}H NMR spectra in $CDCl_3$ are well-defined at 298 K (Figure 5a,c) and complete assignment was achieved thanks to 2D COSY, HMQC, and ROESY NMR experiments (SI). For instance, the β-pyrrolic protons are observed as four AB systems and the protons Ha, Ha′, Hb, and Hb′ as four singlets in the 5−6 ppm region, thus evidencing a dissymmetric structure. The bound acetate anion is observed as a singlet in the high fields (δ = 0.39 and 0.49 ppm for $\mathbf{1}_{Hg}$·**PbOAc,TBA** and $\mathbf{1}_{Cd}$·**PbOAc,TBA**), and integral values confirm that 1 equiv of both TBA^+ and AcO^- belong to the complexes. With Hg(II), a NOE correlation between the CH_3COO protons and a β-pyrrolic proton at 8.99 ppm confirms the positioning of this exogenous ligand above the porphyrin plane. The CONH protons of the strap binding Hg(II) and Cd(II) (NHa′ and NHb′) appear as sharp singlets between 7.70 and 8.10 ppm. In contrast, those of the other strap binding the HAT Pb(II) (NHa and NHb) are broad and downfield-shifted (δ values between 8.75 and 10.0 ppm), which indicates that they are involved in H-bonding interaction with the acetate. Further investigations of the dynamics of these complexes thanks to variable temperature NMR studies are described in section 4.

3. Crystallographic Characterization of the Neutral Heterobimetallic Complexes 1HgPb and 1CdPb and Comparison with Their Related Homobimetallic Complexes $1Pb_2$, $1Hg_2$, and $1Cd_2$. NMR tube solutions of complexes $\mathbf{1}_{Hg}$·**PbOAc** and $\mathbf{1}_{Cd}$·**PbOAc** were subjected to slow evaporation in the presence of few drops of water and dimethyl sulfoxide (DMSO). We were delighted to obtain single crystals for both complexes, which were submitted to X-ray diffraction analysis. The crystallographic structures revealed the formation of the neutral bridged heterobimetallic complexes **1HgPb** and **1CdPb** (Scheme 1 right, Figure 6a,b, and selected distances in Table 1).[28,29] The release of the exogenous acetate has been already observed with the related complexes $\mathbf{1}_{Pb}$·**PbOAc** and $\mathbf{1}_{Cd}$·**CdOAc** upon crystallization or precipitation in polar media, which led to the C_2-symmetric complexes $\mathbf{1Pb_2}$ and $\mathbf{1Cd_2}$.[9d,f]

For both complexes **1HgPb** and **1CdPb**, the porphyrin acts as a bridging ligand with Hg(II)[/Cd(II)] and Pb(II) sitting on each side of the macrocycle. Each metal ion is bound both to the N-core and to the carboxylate group of a strap and undergoes an important OOP displacement (>1.4 Å). Considering the coordination side of the lead cation, several common structural features are observed between **1HgPb** and **1CdPb** (Figure 6b). The lead cation is six-coordinate and located 1.86 Å away from the 24-atom mean plane. First, it is bound to the three nitrogen atoms N1, N2, and N3 of the macrocycle with quite similar bond lengths: N1−Pb = 2.83/2.86 Å, N2−Pb = 2.61/2.63 Å, and N3−Pb = 2.70/2.69 Å for **1HgPb**/**1CdPb**. Second, it is also bound to the intramolecular carboxylate group of the strap and to two DMSO molecules stabilized by H-bonds with the amide groups of the straps (dashed lines in Figure 6a). While the length of the O3(carboxylate)−Pb bond as well as the length of the Os3(DMSO)−Pb bond are similar in both complexes (2.28/2.26 Å and 2.71/2.68 Å), that of the Os4(DMSO)−Pb bond is slightly longer in **1HgPb** (2.80 Å) than in **1CdPb** (2.59 Å). The coordination sphere of the lead cation in these two heterobimetallic complexes can be compared to that of the homobimetallic C_2-symmetric complex $\mathbf{1Pb_2}$ (Figure 6c).[9a] The major difference is represented by the longer length of the N2−Pb σ-bond in **1HgPb**/**1CdPb** (2.61/2.63 Å) vs 2.48 Å in $\mathbf{1Pb_2}$, suggesting that the lead cation is more loosely bound in the heterobimetallic complexes than in the homobimetallic one. This difference is also reflected in the previously mentioned more important OOP distance of the lead cation (1.86 Å in **1HgPb**/**1CdPb** vs 1.79 Å in $\mathbf{1Pb_2}$). Concerning the other side

dx.doi.org/10.1021/ja501926f | J. Am. Chem. Soc. 2014, 136, 6698−6715

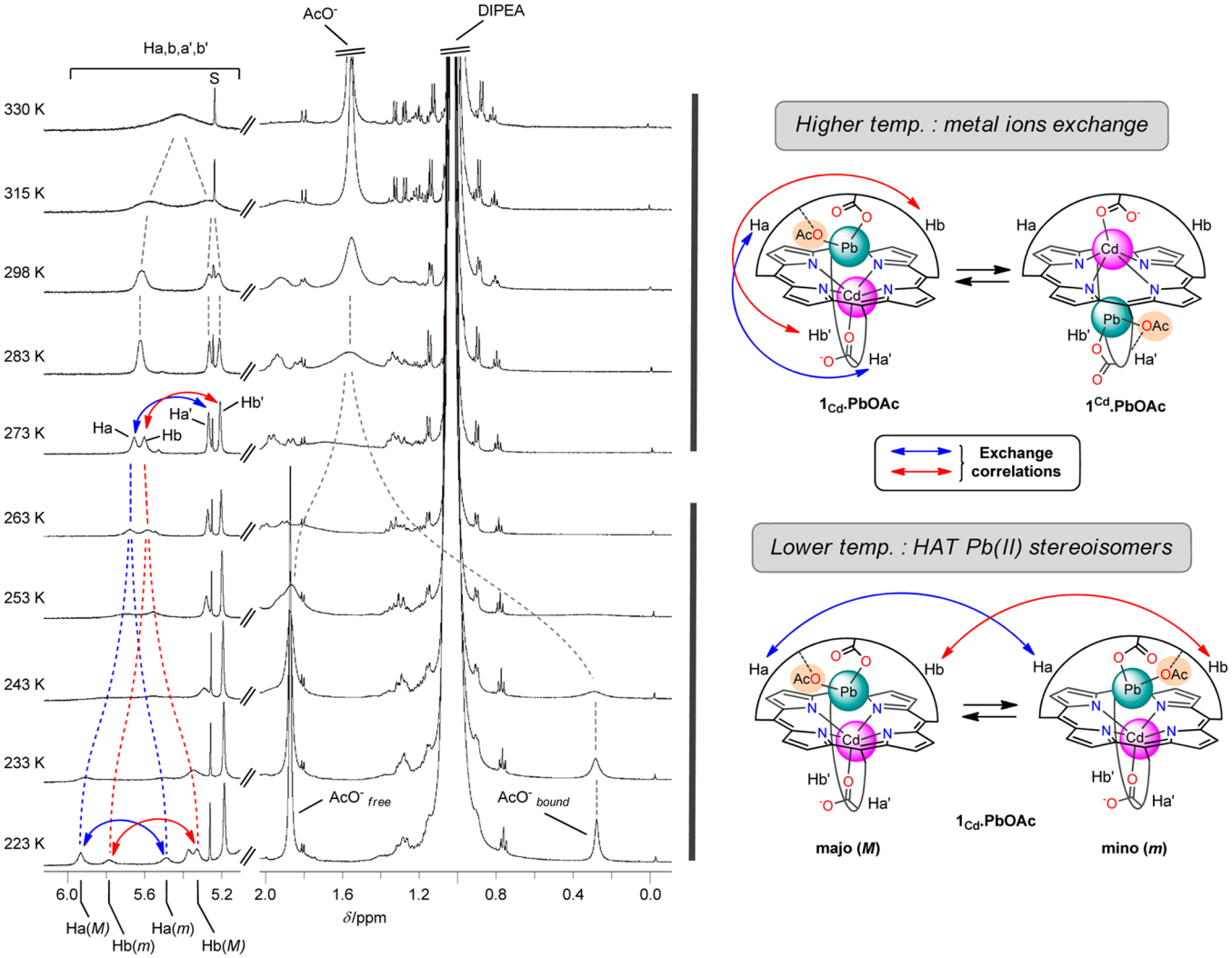

Figure 7. Variable temperature ^{1}H NMR study of $\mathbf{1}_{Cd}$**·PbOAc** (500 MHz, 9:1 $CDCl_3/CD_3OD$, partial spectra), evidencing two different dynamic processes. Sample formed in situ by addition of 1 equiv of $Cd(OAc)_2$ and 1 equiv of $Pb(OAc)_2$ to **1** in the presence of 15 equiv of DIPEA. S = trace of residual solvent.

of the complexes, the Hg and Cd atoms undergo a similar deviation from the mean plane (1.55 and 1.44 Å, respectively). The Hg atom is six-coordinate in **1HgPb**, with three bonds to the N-core of the macrocycle (N1−Hg = 2.44 Å, N3−Hg = 2.66 Å, N4−Hg = 2.44 Å), one bond to the intramolecular carboxylate group (O1−Hg = 2.28 Å), and two bonds with DMSO and methanol molecules (Os1−Hg = 2.70 Å, Os2−Hg = 2.90 Å). Although also six-coordinate, the Cd atom in **1CdPb** displays a different coordination sphere, with four bonds to the N-core of the macrocycle (N1−Cd = 2.39 Å, N2−Cd = 2.55 Å, N3−Cd = 2.53 Å, N4−Cd 2.38 Å), one bond to the intramolecular carboxylate group (O1−Cd = 2.30 Å), and one bond with a methanol molecule (Os2−Cd = 2.61 Å). The DMSO and methanol molecules bound to Hg and Cd are also stabilized by H-bonds with the amide groups of the straps (dashed lines in Figure 6a).

The present structures of **1HgPb**/**1CdPb** can also compare with the structures of the corresponding homobimetallic complexes $\mathbf{1Hg_2}$ and $\mathbf{1Cd_2}$ (Figure 6c).[9b,f] In the case of $\mathbf{1Hg_2}$, a dissymmetric complex in the solid state, the mercury cation labeled Hg2 is the most similar to Hg in **1HgPb** (both are six-coordinate). However, the OOP displacement of the mercury cation in **1HgPb** (1.55 Å) is roughly midway as compared to those in $\mathbf{1Hg_2}$ (1.41 and 1.73 Å). A main difference consists of the two σ-bonds of the mercury cations that are much longer in **1HgPb** (2.44/2.28 Å) than in $\mathbf{1Hg_2}$ (2.16/2.10 and 2.13/2.07 Å), with a different spatial arrangement. They are in a trans geometry in $\mathbf{1Hg_2}$ (N2−Hg1−O1 = 166°; N4−Hg2−O3 = 161°), whereas a cis arrangement is observed in **1HgPb** (N4−Hg−O1 = 85°), a more unusual coordination geometry for mercury. Concerning the cadmium complexes, the Cd atoms undergo similar deviations from the mean plane (1.44 Å vs 1.44/1.51 Å). It is worthwhile to note that two of the four N−Cd bonds are shorter in **1CdPb** (2.38/2.39 Å vs 2.53/2.55 Å), whereas the N−Cd distances are almost equivalents in $\mathbf{1Cd_2}$. This shortening is accompanied by a more pronounced tilting of the pyrroles in **1CdPb** than in $\mathbf{1Cd_2}$. From these X-ray data, it can be deduced that the strongest tilting of the pyrrole ring is proportional to the size of the cation [Pb(II) > Hg(II) > Cd(II)] with almost no tilting for the homobimetallic cadmium complex (1.8° and 2.4°) and a strong one for the homobimetallic lead complex (11°).

These five X-ray structures evidence the remarkable propensity of ligand **1** for bridging two divalent heavy metal ions. A selective access to the neutral heterobimetallic complexes remains delicate in solution, which highlights this

dx.doi.org/10.1021/ja501926f | J. Am. Chem. Soc. 2014, 136, 6698−6715

Scheme 2. Comparison of the Dynamic Features of the Heterobimetallic Complexes 1_{Hg}·PbOAc and 1_{Cd}·PbOAc[a] (b) with the Related HAT Pb(II) Bimetallic Complexes 1_{Bi}·PbOAc[9d] (a) and 1_{Pb}·PbOAc[9d] (c)

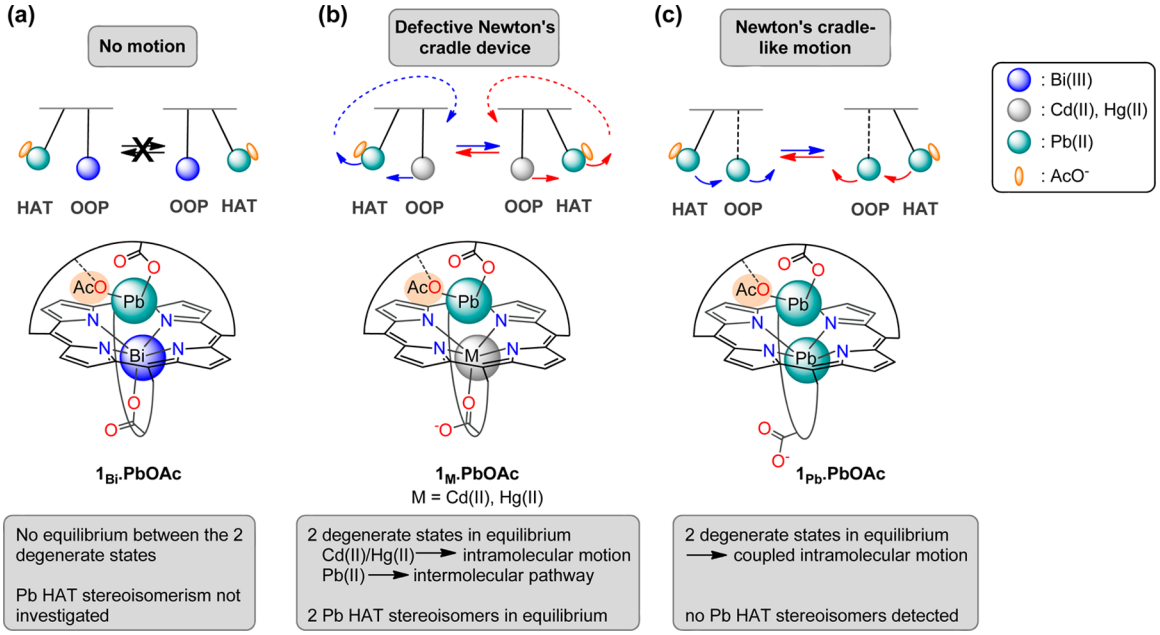

[a]The complexes are formed in situ in a 9:1 $CDCl_3/CD_3OD$ mixture in the presence of DIPEA. HAT and OOP stand for hanging-atop and out-of-plane.

two-step process via the HAT Pb(II) heterobimetallic complexes (Scheme 1, right).

4. Dynamic Study of the Heterobimetallic Complexes 1_{Hg}·PbOAc and 1_{Cd}·PbOAc. Next, we have investigated the dynamic behavior of the complexes **1_{Hg}·PbOAc** and **1_{Cd}·PbOAc** under two sets of conditions: (i) first, with the complexes formed in situ by addition of 1 equiv of each acetate metal salt, in a $CDCl_3/CD_3OD$ 9:1 mixture with 15 equiv of DIPEA, which generates 3 equiv of free acetate anions in a slightly polar medium and (ii) second, with the analytical samples (TBA^+ salts) in pure $CDCl_3$ solution, therefore with no excess of acetate anions in an apolar medium.

In the first conditions, a variable temperature ^1H NMR experiment conducted with **1_{Cd}·PbOAc** evidenced two sets of dynamic behaviors (Figure 7 and SI). Starting from 298 K, increasing the temperature led to a coalescence of the signals, and a C_2-symmetric pattern was observed above 330 K (Figure 7, upper part and SI). At the opposite, lowering the temperature led to a splitting of the signals and to the appearance of two dissymmetric NMR patterns, in a ca. 2:1 ratio at 223 K (Figure 7, lower part). Both dynamic processes were analyzed by 2D ROESY NMR experiments performed at 283 and 223 K (SI), allowing unambiguous assignments of some characteristic resonances (selected exchange correlations depicted in Figure 7). The coalescence of, for instance, Ha−Ha′ and Hb−Hb′ at high temperature indicates that both metal ions invert their positions relative to the mean plane of the macrocycle and thus migrate concomitantly from one to the other side of the porphyrin. In other words, there is an equilibrium between the two degenerate states **1_{Cd}·PbOAc** and **1^{Cd}·PbOAc**, as depicted in Figure 7 (top). The same exchange correlations were observed at 298 K with **1_{Hg}·PbOAc**, showing that such equilibrium between the two degenerate states also occurs with this complex (SI). Conversely, when similar variable temperature ^1H NMR studies were conducted in the second set of conditions with both complexes, neither coalescence at high temperature nor exchange correlations between, for example, Ha and Ha′ protons were observed (2D ROESY NMR experiments at 298 K, SI). These NMR data indicate that, in the absence of free AcO^- in the medium, there is no equilibrium between the degenerate states of **1_{Cd}·PbOAc,TBA** and **1_{Hg}·PbOAc,TBA**. Thus, a plausible mechanism for the metal exchange process would involve the following steps: (i) An intermolecular pathway has to be considered for the large Pb(II) ion, which requires the presence of an excess of AcO^-, allowing the release of $Pb(OAc)_2$. (ii) An intramolecular pathway for Cd(II)/Hg(II) is likely to occur, with migration of these ions from one to the other side of the porphyrin through the N-core; such a dynamic was observed in the case of the corresponding monometallic complexes **1^{Hg}** and **1^{Cd}** (simplified structures in Figure 4).[9b,f] The sharpening of their $^{199}Hg/^{113}Cd$ signal upon complexation of the HAT Pb(II) (Figure 4a,b) is in line with a slower funneling motion of Hg(II)/Cd(II) in the heterobimetallic complexes. (iii) A released $Pb(OAc)_2$ is bound by the other overhanging COO^-.

This double translocation process of two different metal ions differs from the recently described Newton's cradle-like motion observed with the related homobimetallic complexes **1_{Pb}·PbOAc**, **1_{Bi}·Bi(OAc)$_2$**, and **1_{Cd}·CdOAc**.[9d,f] In the Newton's cradle-like motion, equilibrium between the two degenerate states, e.g. **1_{Pb}·PbOAc** and **1^{Pb}·PbOAc**, involves a coupled intramolecular migration of the metal ions that stay on their respective sides of the porphyrin (compartmentalized motion; see Scheme 2c). With the heterobimetallic complexes, such a motion would lead to a different complex (a coordination isomer such as, for example, **1_{Pb}·CdOAc**, with Pb(II) bound to the N-core and CdOAc bound to the strap) and is not observed. There is indeed a high selectivity in favor of the smaller ions Hg(II) and Cd(II) for the N-core and of the larger one Pb(II) for the strap. The double translocation according to

dx.doi.org/10.1021/ja501926f | J. Am. Chem. Soc. 2014, 136, 6698−6715

Scheme 3. Illustration of the On/Off Controlled Equilibrium between the Two Degenerate States 1_{Cd}·PbOAc and 1^{Cd}·PbOAc Mediated by a Catalytic Amount of a Chemical Effector (AcO^-TBA^+)

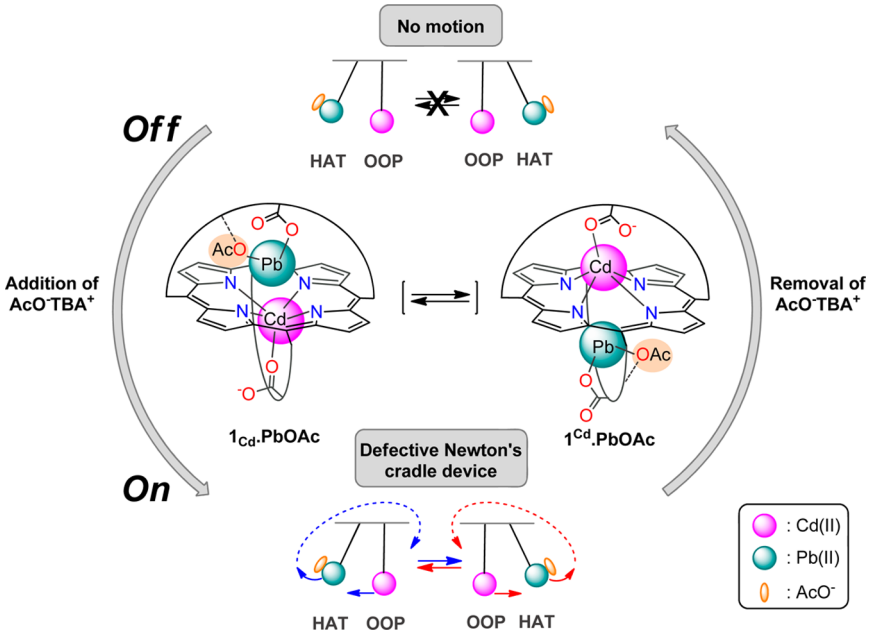

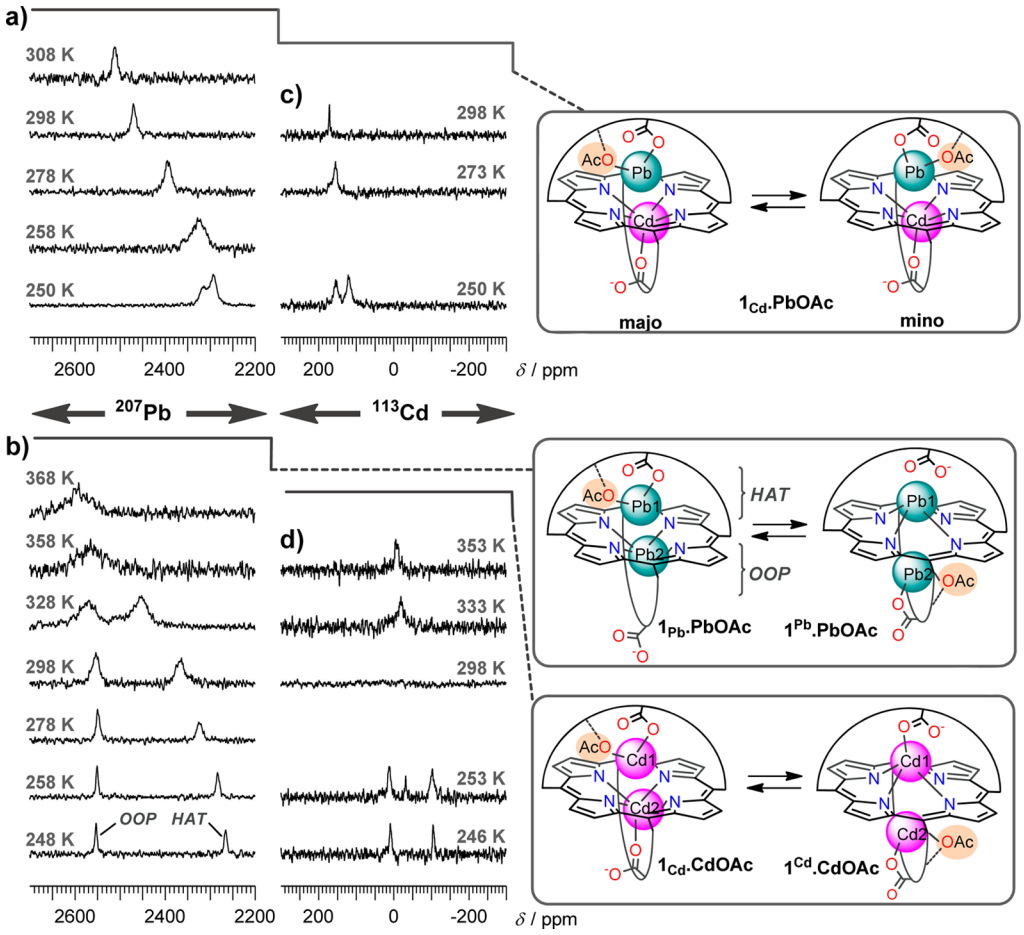

Figure 8. Variable temperature ^{207}Pb and ^{113}Cd heteronuclear NMR study of $\mathbf{1_{Cd}}$**·PbOAc** and comparison with $\mathbf{1_{Pb}}$**·PbOAc** and $\mathbf{1_{Cd}}$**·CdOAc**[9f] (9:1 $CDCl_3/CD_3OD$, 9.4 T): (a and b) ^{207}Pb NMR spectra of $\mathbf{1_{Cd}}$**·PbOAc** and $\mathbf{1_{Pb}}$**·PbOAc**, respectively, at various temperatures and (c and d) ^{113}Cd NMR spectra of $\mathbf{1_{Cd}}$**·PbOAc** and $\mathbf{1_{Cd}}$**·CdOAc**, respectively, at various temperatures. The samples were formed in situ by addition of stoichiometric amounts of the corresponding acetate metal salts in the presence of 7.5 equiv of DIPEA. HAT and OOP stand for hanging-atop and out-of-plane, respectively.

dx.doi.org/10.1021/ja501926f | J. Am. Chem. Soc. 2014, 136, 6698−6715

a mixed intermolecular [relative to Pb(II)] and intramolecular [relative to Cd(II)/Hg(II)] pathway leads however to a situation similar to that observed with the homobimetallic complexes, with metal ions alternatively hanging-atop and out-of-plane on one side of the porphyrin. Such a process can be seen as a peculiar motion of a defective Newton's cradle device, as it allows the sphere 1 to replace sphere 2, which is impossible in a macroscopic Newton's cradle (Scheme 2b). It is worth mentioning that with the related heterobimetallic complex $\mathbf{1_{Bi}}$·**PbOAc**,[9d] no equilibrium between its two degenerate states is observed (Scheme 2a). This is due to the large ionic radius and high affinity of the trivalent metal ion that prevent both an intramolecular pathway via funneling through the N-core and an intermolecular pathway via a release process. This comparison in Scheme 2 highlights how the dynamics of these HAT Pb(II) bimetallic complexes drastically depends on the nature of the N-core-bound metal ion.

Interestingly, this motional dynamics of the metal ions can be switched on and off (Scheme 3). Indeed, starting from an analytical sample of $\mathbf{1_{Cd}}$·**PbOAc,TBA** in pure $CDCl_3$ (second set of conditions), the addition of a catalytic amount of AcO^-TBA^+ (0.1 equiv) led to the appearance of exchange correlations between, for instance, Ha−Ha′ and Hb−Hb′ protons in the corresponding 2D ROESY NMR spectrum (SI), thus evidencing an equilibrium between the degenerate states. Removal of this excess of AcO^-TBA^+ upon precipitation of the sample with pentane led back to the absence of exchange correlations. It is thus possible to switch between an active and an inactive state of a defective Newton's cradle device by addition and removal of a chemical effector (Scheme 3).

The second dynamic process observed at low temperature with $\mathbf{1_{Cd}}$·**PbOAc** (Figure 7, lower part) also took place with $\mathbf{1_{Hg}}$·**PbOAc**, with two dissymmetric NMR patterns observed at 223 K, in a ca. 95:5 ratio (SI, first set of conditions). 2D ROESY NMR experiments were performed at low temperatures (SI) and revealed that, for both complexes, the Ha and Hb protons are significantly affected upon splitting as compared to Ha′ and Hb′, with $\Delta\delta$ up to ca. 0.4 ppm between the major and minor species (selected exchange correlations are indicated by blue and red arrows in Figure 7 for $\mathbf{1_{Cd}}$·**PbOAc**; splitting highlighted by blue and red dashed lines). Further investigations were limited by the significant broadening of the NMR patterns at low temperatures. Variable temperature ^{207}Pb and ^{113}Cd heteronuclear NMR studies were thus undertaken with $\mathbf{1_{Cd}}$·**PbOAc** (Figure 8a,c). For both nuclei, a splitting is observed at low temperatures: at 250 K, the ^{207}Pb NMR spectrum showed two overlapping signals at 2313 and 2293 ppm, and the ^{113}Cd spectrum revealed two well-resolved signals at 154 and 120 ppm (parts a and c of Figure 8, respectively). The relatively small $\Delta\delta$ values of respectively 20 and 33 ppm contrast with those of the related homobimetallic complexes $\mathbf{1_{Pb}}$·**PbOAc** and $\mathbf{1_{Cd}}$·**CdOAc** (parts b and d of Figure 8, respectively), for which significant differences between the HAT and OOP resonances are observed under similar experimental conditions ($\Delta\delta_{HAT-OOP} \sim 289$ and 113 ppm for $\mathbf{1_{Pb}}$·**PbOAc** and $\mathbf{1_{Cd}}$·**CdOAc**, respectively). These data indicate minor differences in the coordination modes of Cd(II) and Pb(II) in the heterobimetallic complex at low temperature, the metal ions staying respectively bound to the N-core and to the strap.

Deeper insights into this low-temperature dynamic behavior came from variable temperature ^{1}H NMR experiments conducted with the analytical samples (second set of conditions). Rather unexpectedly, $\mathbf{1_{Hg}}$·**PbOAc,TBA** and $\mathbf{1_{Cd}}$·**PbOAc,TBA** also gave rise to two species with dissymmetric NMR patterns at 213 K, in respectively 15:1 and 1.5:1 ratios (Figure 5b,d and SI). This indicates that free acetates are not required for this dynamic process. For $\mathbf{1_{Cd}}$·**PbOAc,TBA**, the CH_3 protons of the bound acetate are observed at 0.43 and 0.40 ppm for the major and minor species, which confirms little differences in the coordination mode of the HAT Pb(II) ion (Figure 5d). Assignment of characteristic signals was also realized thanks to 2D ROESY NMR experiments (SI). For instance, with $\mathbf{1_{Cd}}$·**PbOAc,TBA**, a NOE correlation between the CH_3 protons of the bound acetate and one of the four NHCO protons of the straps allowed unambiguous localization of the H-bonding interaction stabilizing the HAT Pb(II) metal ion. Interestingly, for the major and minor species, opposite NHCO protons of a strap are involved in the second sphere of coordination with PbOAc: the NHa proton (δ = 10.62 ppm) for the major and the NHb proton (δ = 10.41 ppm) for the minor (see also values in Figure 5 for $\mathbf{1_{Hg}}$·**PbOAc,TBA**). All of these data indicate the presence of two HAT Pb(II) diastereoisomers that differ by the orientation of the PbOAc moiety H-bound either to the left or right side of the strap (see structures in Figure 5).[30] Equilibrium between these stereoisomers is expected to follow an intramolecular pathway, i.e., via a swinging motion of PbOAc oscillating between the two sides of the strap. It is worth noting that the $\Delta\delta$ value between NHa and NHb is more important with the major diastereoisomer than with the minor one ($\Delta\delta_M$ = 2.84 vs $\Delta\delta_m$ = 2.28 ppm for $\mathbf{1_{Hg}}$·**PbOAc,TBA** and $\Delta\delta_M$ = 2.54 vs $\Delta\delta_m$ = 2.10 ppm for $\mathbf{1_{Cd}}$·**PbOAc,TBA**; see Figure 5). This is consistent with a stronger H-bonding interaction with the major isomers. It is also interesting to mention that the difference between these $\Delta\delta$ value (i.e., $\Delta\delta_M - \Delta\delta_m$) is more important with Hg(II) vs Cd(II) (0.56 vs 0.44 ppm; see Figure 5). These data also reflect the higher diastereoselectivity observed with Hg(II) bound to the N-core vs Cd(II) (M/m ratio of 15:1 vs 1.5:1, respectively) and evidence an effective communication between the two sides of the porphyrin ligand. In the case of $\mathbf{1_{Pb}}$·**PbOAc**, such a stereoisomerism was not observed at low temperatures, which might indicate a highly selective formation of a single HAT Pb(II) diastereoisomer.

To summarize this dynamic study, the complexes $\mathbf{1_{Hg}}$·**PbOAc** and $\mathbf{1_{Cd}}$·**PbOAc** are obtained as two HAT Pb(II) diastereoisomers that undergo an inherent equilibrium, likely via a swinging of PbOAc between the left and right sides of its binding strap ($\Delta G^{\ddagger} \approx 11.2$ kcal mol^{-1} with Cd(II), SI). A second dynamic behavior with a higher activation energy also takes place ($\Delta G^{\ddagger} \approx 15.1$ kcal mol^{-1} with Cd(II), SI) and consists of an equilibrium between two degenerate states. It occurs via a double translocation of the two metal ions according to a mixed intra- and intermolecular pathway and is controlled by the presence of excess of AcO^- in the medium. Compared to the related homobimetallic complexes, such a motional dynamics corresponds to a peculiar motion of spheres in a defective Newton's cradle device. Its frequency is lower than the Newton's cradle-like motion of Pb(II) and Cd(II) in $\mathbf{1_{Pb}}$·**PbOAc** ($\Delta G^{\ddagger} \approx 13.7$ kcal mol^{-1})[9d] and $\mathbf{1_{Cd}}$·**CdOAc** ($\Delta G^{\ddagger} \approx 11.5$ kcal mol^{-1}),[9f] which is likely due to the intermolecular exchange of Pb(II).

5. Dynamic Constitutional Evolution as a Means To Control Metal Migration Processes. In the previous sections, the heterobimetallic complexes $\mathbf{1_{Hg}}$·**PbOAc** and $\mathbf{1_{Cd}}$·**PbOAc** were formed by addition of the corresponding acetate

dx.doi.org/10.1021/ja501926f | J. Am. Chem. Soc. 2014, 136, 6698−6715

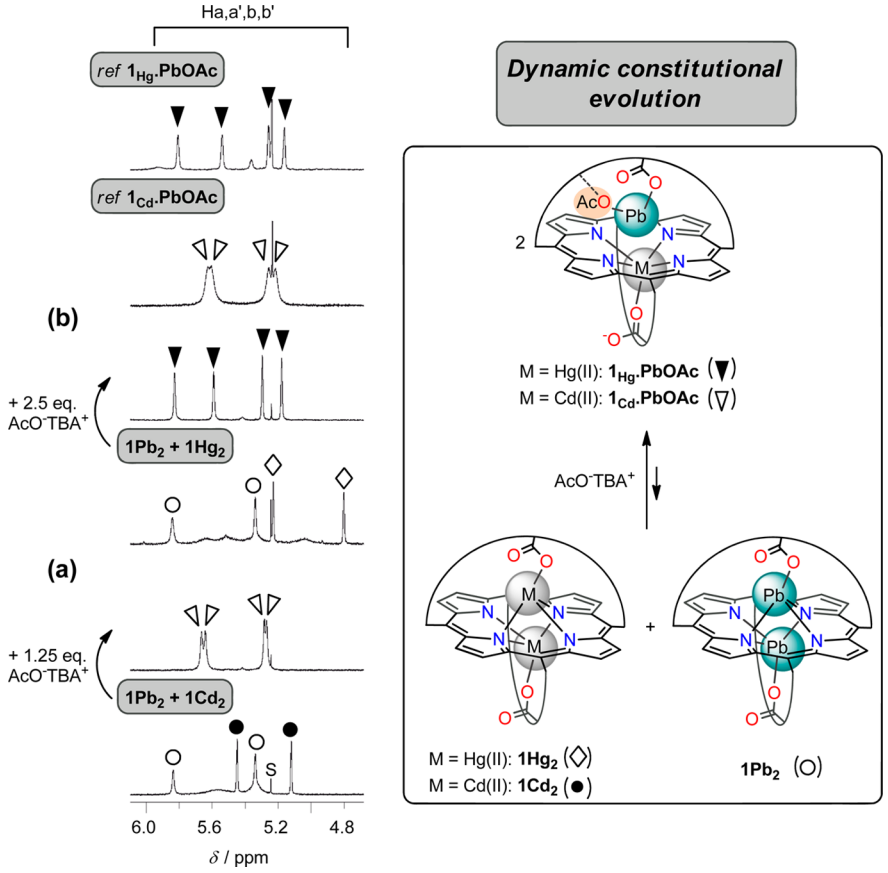

Figure 9. Partial ^{1}H NMR spectra (298 K, 500 MHz, $CDCl_3/CD_3OD$ 9:1) of a 1:1 mixture of $\mathbf{1Pb_2}$ and either $\mathbf{1Cd_2}$ (a) or $\mathbf{1Hg_2}$ (b), before and after addition of a slight excess of AcO^-TBA^+. Top: reference spectra of the heterobimetallic complexes $\mathbf{1_{Hg}}$**·PbOAc** and $\mathbf{1_{Cd}}$**·PbOAc** formed in situ by addition of 1 equiv of the corresponding acetate metal salts to **1**, in the presence of 15 equiv of DIPEA. For proton labeling, see Scheme 1. S = trace of residual solvent.

metal salts to **1**. During the course of our investigations, we have observed that these complexes could be successfully obtained via another strategy, as revealed by the ^{1}H NMR experiment of Figure 9: starting from a 1:1 mixture of $\mathbf{1Pb_2}$ and either $\mathbf{1Hg_2}$ or $\mathbf{1Cd_2}$ (analytical samples) in a 9:1 $CDCl_3/CD_3OD$ mixture, addition of a slight excess of tetrabutylammonium acetate (AcO^-TBA^+) led quantitatively to $\mathbf{1_{Hg}}$**·PbOAc** and $\mathbf{1_{Cd}}$**·PbOAc** (instantaneous process at 298 K). The HAT Pb(II) complexation thus appears as a strong driving force that is responsible for a full displacement of equilibrium from a mixture of two homobimetallic complexes (virtually $\mathbf{1Hg_2}/\mathbf{1_{Cd}}$**·CdOAc** and $\mathbf{1_{Pb}}$**·PbOAc**) to a single heterobimetallic complex. In other words, this experiment evidenced a constitutional evolution of a dynamic library of bimetallic complexes triggered by the addition of a chemical effector (AcO^-). To the best of our knowledge, dynamic libraries based on metal ion exchange with metalloporphyrins are unprecedented. These results, although obtained with a minimal library of three members (two homo- and one heterobimetallic complexes), clearly establish a proof of concept. In principle, all the various bimetallic mixtures of **1** discussed in section 1 could be subjected to dynamic constitutional evolution.

We have further investigated the concept of dynamic constitutional evolution with $\mathbf{1_{Hg}}$**·PbOAc** as a means to control metal ions migration processes. An analytical sample of this complex (TBA^+ salt) was dissolved in a 9:1 $CDCl_3/CD_3OD$ solution, and an excess of dimethylaminopyridine (DMAP) was added at 298 K (up to 115 equiv, Figure 10a). This led to the appearance of the homobimetallic complexes $\mathbf{1Hg_2}$**·DMAP** and $\mathbf{1_{Pb}}$**·PbOAc**. To our delight, these two complexes (1:1 ratio) were the only observed species at a lower temperature (263 K, Figure 10a), evidencing a highly selective amplification process. The further addition of 25 equiv of AcO^-TBA^+ at 298 K led back quantitatively to $\mathbf{1_{Hg}}$**·PbOAc** (Figure 10a). This experiment nicely shows a full control of the formation of homo- vs heterobimetallic species relying on a dynamic constitutional evolution process triggered forward and backward by two different chemical effectors.

As revealed by ^{199}Hg heteronuclear NMR experiments (Figure 11), the selective interaction of DMAP with $\mathbf{1Hg_2}$ is at the origin of the evolution of the mixture. We have previously shown that DMAP can induce a positive cooperativity for the formation of $\mathbf{1Hg_2}$ due to its preferential interaction with the bimetallic complex (deduced from ^{1}H NMR titration experiments).[9b] To illustrate this effect, an excess of DMAP was added to the monometallic complex $\mathbf{1^{Hg}}$, which led to a shift of the equilibria toward the formation of **1** and $\mathbf{1Hg_2}$**·DMAP** (Figure 11b; ^{1}H NMR monitoring in the SI). The latter complex is characterized by a single resonance at −1865 ppm, vs −1360 ppm for $\mathbf{1^{Hg}}$ and −2004 ppm for $\mathbf{1Hg_2}$ (Figure 11a). Similarly, addition of DMAP to $\mathbf{1_{Hg}}$**·PbOAc** led to the appearance of the signal of $\mathbf{1Hg_2}$**·DMAP** (constitutional evolution of the mixture), whereas the signal of the heterobimetallic complex was not affected (δ = −1741 ppm; Figure 11c). These data evidence that DMAP interacts selectively with the Hg(II) ions of the homobimetallic complex

dx.doi.org/10.1021/ja501926f | J. Am. Chem. Soc. 2014, 136, 6698−6715

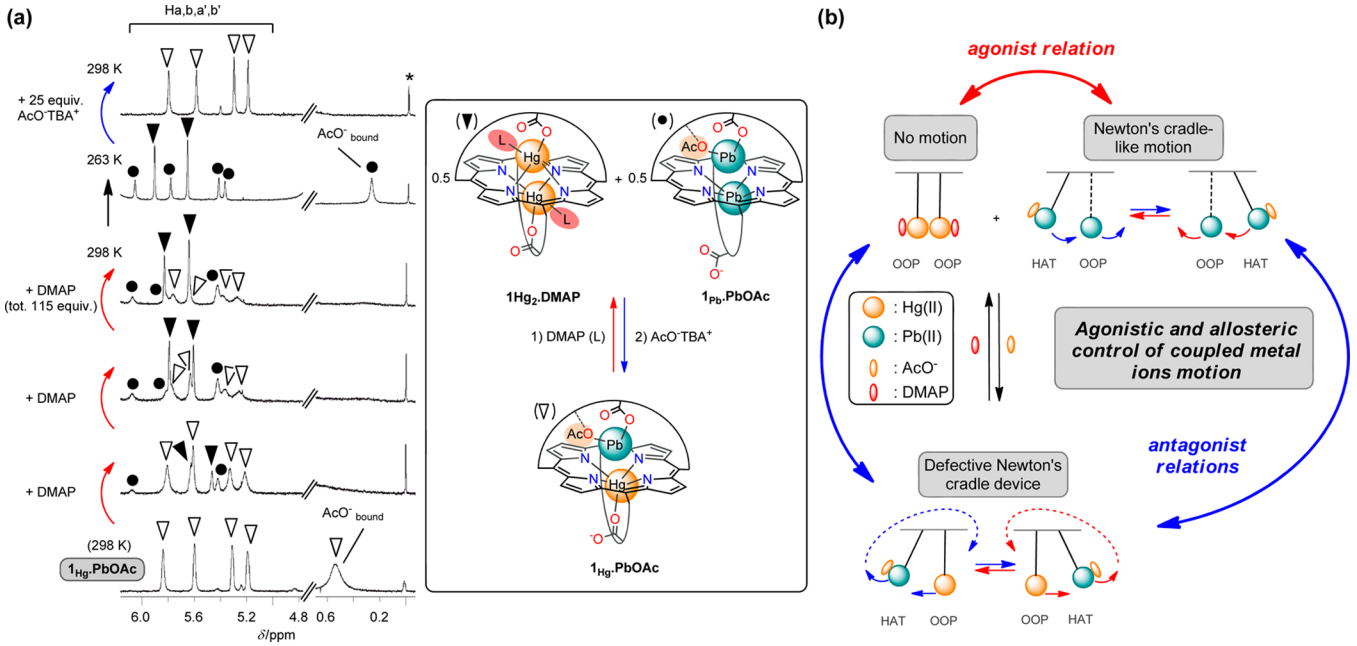

Figure 10. (a) ^{1}H NMR study (9:1 $CDCl_3/CD_3OD$, 500 MHz, partial spectra) evidencing a full switching between the hetero and homo Pb(II)/Hg(II) bimetallic complexes of **1** (from bottom to top): (1) successive additions of DMAP to $\mathbf{1_{Hg}}$**·PbOAc,TBA** leads, upon cooling to 263 K, to a 1:1 mixture of $\mathbf{1Hg_2}$**·DMAP** and $\mathbf{1_{Pb}}$**·PbOAc**; (2) back to 298 K, the further addition of excess of AcO^- leads to full recovery of $\mathbf{1_{Hg}}$**·PbOAc** ("*" indicates the residual signal of grease). (b) Control of metal ions migration processes in Pb(II)/Hg(II) bimetallic complexes of **1**: indirect agonistically enforced amplification of $\mathbf{1_{Pb}}$**·PbOAc** through up-regulation of its agonist $\mathbf{1Hg_2}$**·DMAP** by addition of a chemical effector (DMAP). HAT and OOP stand for hanging-atop and out-of-plane, respectively.

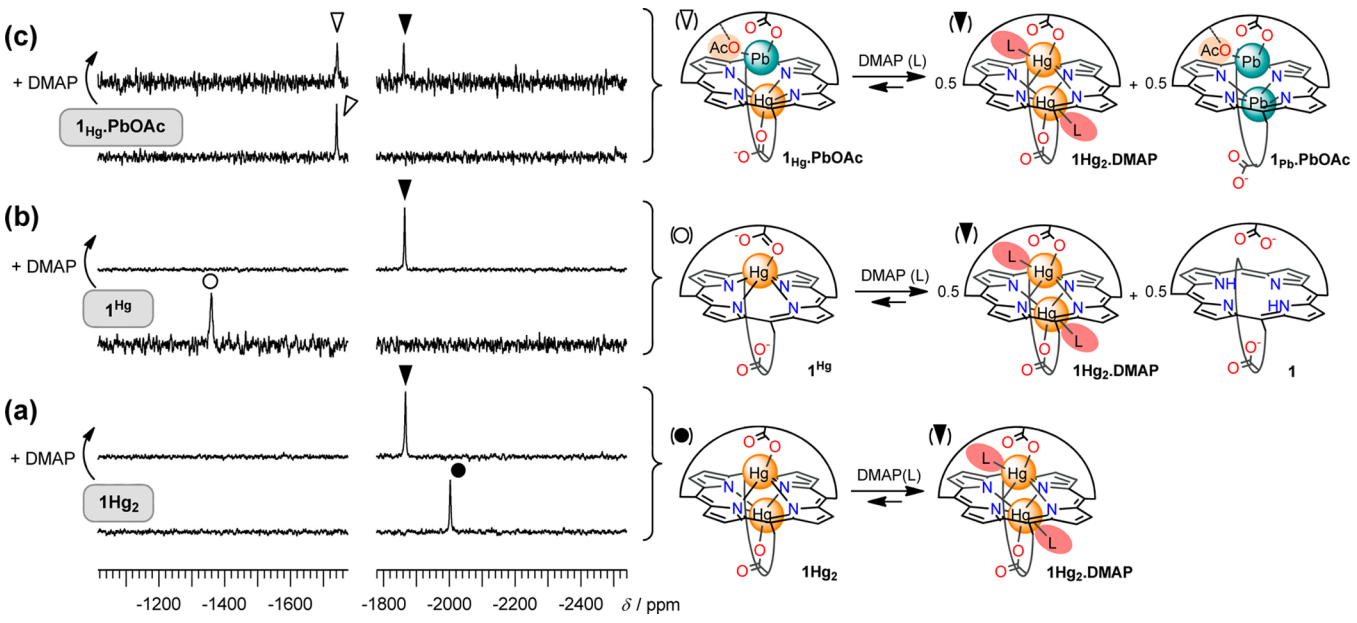

Figure 11. ^{199}Hg heteronuclear NMR study (9:1 $CDCl_3/CD_3OD$, 9.4 T, 298 K, with 7.5 equiv of DIPEA) related to the influence of DMAP on various Hg(II) complexes of **1**: (a) $\mathbf{1Hg_2}$, (b) $\mathbf{1}^{Hg}$, and (c) $\mathbf{1_{Hg}}$**·PbOAc** before and after addition of excess of DMAP.

vs the Hg(II) ion of the heterobimetallic one. The reason for that is the strong coordination of the overhanging carbonyl group to the Hg atom bound to the N-core in $\mathbf{1_{Hg}}$**·PbOAc** (see the structure in Scheme 1), against which DMAP has to compete.

The formation of $\mathbf{1_{Pb}}$**·PbOAc** is not due to its interaction with DMAP[31] but occurs thanks to its agonist relation with $\mathbf{1Hg_2}$**·DMAP**, and both homobimetallic complexes have an antagonist relation with the heterobimetallic one (Figure 10b). Thus, the formation of $\mathbf{1_{Pb}}$**·PbOAc** upon addition of DMAP to $\mathbf{1_{Hg}}$**·PbOAc** is an indirect amplification process, agonistically driven. The most likely explanation for the way back to $\mathbf{1_{Hg}}$**·PbOAc** is that only half of the 1:1 mixture of the homobimetallic complexes interacts with AcO^-, whereas the full mixture interacts with AcO^- upon formation of the heterobimetallic complex. Thus, the equilibrium is shifted back to the situation allowing a higher amount of AcO^- to be consumed.[32]

dx.doi.org/10.1021/ja501926f | J. Am. Chem. Soc. 2014, 136, 6698−6715

From the aspect of the metal ions motion in the different complexes, it is thus possible to switch forward and backward between two different coupled migration processes, i.e., between the peculiar motion of a defective Newton's cradle device and the compartmentalized Newton's cradle-like motion, respectively, in $\mathbf{1}_{Hg}$·**PbOAc** and $\mathbf{1}_{Pb}$·**PbOAc**. Considering the latter complex, the coupled motion of the metal ions is under both allosteric and agonistic control. Thus, in the future, dynamic constitutional evolution could become a means to control the functioning of related adaptative machines.

CONCLUSION

Combined ^{1}H and heteronuclear NMR studies have unraveled unique dynamic behaviors with Pb(II)/Hg(II) and Pb(II)/Cd(II) heterobimetallic complexes of a bis-strap porphyrin ligand. Dynamic processes occur at three different levels (strap, ligand, and library of complexes), and they can be summarized as follows:

(1) $\mathbf{1}_{Hg}$·**PbOAc** and $\mathbf{1}_{Cd}$·**PbOAc** exist as two diastereoisomers inherently in equilibrium. The PbOAc moiety likely swings between the left and right sides of its binding strap, due to a second sphere of coordination with the lateral non-equivalent NHCO groups.

(2) $\mathbf{1}_{Hg}$·**PbOAc** and $\mathbf{1}_{Cd}$·**PbOAc** also exist as two degenerate states, and equilibrium between these two states can be turned on and off by addition and removal of a chemical effector (AcO^-). The exchange process corresponds to a double translocation of the two metal ions, with an intramolecular migration of Hg(II)[/Cd(II)] through the N-core coupled to an intermolecular pathway for PbOAc (formally, N-core^{up} ⇆ N-core^{down} coupled to strap^{down} ⇆ strap^{up}). It contrasts with the double translocation process observed with the related Bi(III), Pb(II), and Cd(II) homobimetallic complexes, which involves an intramolecular coupled migration of the two metal ions (strap^{up} ⇆ N-core^{up} coupled to N-core^{down} ⇆ strap^{down}). Thus, the heterobimetallic complexes behave as defective Newton's cradle devices (the metal ions migrate from one to the other side of the porphyrin), as compared to the homobimetallic ones, in which the metal ions motion is compartmentalized, similarly to a macroscopic Newton's cradle device.

(3) The third level involves equilibrium between hetero- and homobimetallic complexes that can be fully shifted forward and backward by addition of two different chemical effectors. Such a behavior corresponds to a reversible dynamic constitutional evolution of the system upon successive modifications of the environment. The hetero- and homobimetallic complexes associated with a pair of metal ions thus form a dynamic library of three members able to undergo self-organization processes. In the present case, dynamic constitutional evolution allows one to switch between the two above-mentioned double translocation processes (the second level of dynamics), thanks to an indirect (agonistic) amplification process.

In addition to that, the neutral heterobimetallic complexes **1HgPb** and **1CdPb** have been structurally characterized. Such bridged complexes with two different metal ions bound to the N-core have been scarcely reported.[11]

These results further establish a new approach in supramolecular coordination chemistry with metalloporphyrins, by considering the reversible interaction of metal ions with the porphyrin N-core as a new source of self-organization processes. They open the way to the formation of adaptative materials and devices that would display specific properties or functions associated with a given constitution of the bimetallic complexes. Work is these directions is in progress in our laboratories.

EXPERIMENTAL SECTION

General. All of the NMR experiments were conducted in 5 mm standard NMR tubes. ^{1}H NMR spectra were recorded at 500 MHz. Chemical shifts are expressed in parts per million, and traces of residual solvents were used as internal standards. All of the ^{1}H NMR signals were assigned using 2D NMR experiments (COSY, HMQC, ROESY). Compound **1** was prepared as previously described.[9a] All of the chemicals were commercial products and used as received.

^{113}Cd, ^{199}Hg, and ^{207}Pb Heteronuclear NMR Experiments. Natural abundance ^{113}Cd, ^{199}Hg, and ^{207}Pb NMR spectra were recorded on a spectrometer equipped with temperature regulation, operating at 9.4 T (88.7, 71.6, and 83.6 MHz, respectively), using a 5 mm automated triple broadband probe. The samples were prepared at a 2.2×10^{-2} M concentration of ligand, in a 9:1 $CDCl_3/CD_3OD$ mixture, following the typical procedure described below for the ^{1}H NMR experiments. The samples were left to reach equilibrium at the desired temperature within the magnet for at least 10 min before the NMR measurements. All the heteronuclear NMR spectra were recorded with the improved RIDE (ring down elimination) pulse sequence of Kozminsky et al., which has been proven to dramatically improve the baseline of ^{17}O, ^{29}Si, and ^{113}Cd spectra.[33,9f] The ^{113}Cd spectra were recorded using the following acquisition parameters: spectral width of about 940 ppm (83.3 kHz), 15 ms relaxation delay, 5 ms acquisition time, 90° excitation pulse, and a number of transients ranging between 4.0×10^3 and 8.2×10^4. The ^{199}Hg spectra were recorded using the following acquisition parameters: spectral width of about 832 ppm (59.5 kHz), 0.5 s relaxation delay, 50 ms acquisition time, 90° excitation pulse, and a number of transients ranging between 3.3×10^3 and 4.9×10^4. The ^{207}Pb spectra were recorded using the following acquisition parameters: spectral width of about 996 ppm (83.3 kHz), 0.15 s relaxation delay, 5 ms acquisition time, 90° excitation pulse, and a number of transients ranging between 3.6×10^3 and 3.4×10^5. The spectra were recorded lock-on without sample spinning. The processing comprised exponential multiplication of the FID with a line broadening factor of 100 Hz, zero-filling, Fourier transform, zero-order phase correction, baseline correction, and correction of the free induction decay (FID) by backward linear prediction. The ^{113}Cd chemical shift scale was calibrated at 298 K with respect to an external 0.1 M sample of $Cd(ClO_4)_2$ in D_2O (0 ppm).[34] The ^{199}Hg chemical shift scale was calibrated at 298 K with respect to an external 1 M sample of $Hg(OAc)_2$ in CD_3CO_2D (−2389.0 ppm).[35] The ^{207}Pb chemical shift scale was calibrated at 298 K with respect to an external 1 M sample of $Pb(NO_3)_2$ in D_2O (0 ppm).[36]

^{1}H NMR Titration Experiments—Typical Procedure for the Formation of $\mathbf{1}_{Cd}$·PbOAc. The complex was prepared by mixing 3.0 mg of **1** (2.38 μmol), 500 μL of 9:1 $CDCl_3/CD_3OD$, 6 μL of DIPEA (34.4 μmol, 15 equiv), 40 μL (2.37 μmol, 1 equiv) of a stock solution of $Cd(OAc)_2{\cdot}2H_2O$ (7.9 mg in 500 μL of 9:1 $CDCl_3/CD_3OD$), and 40 μL (2.38 μmol, 1 equiv) of a stock solution of $Pb(OAc)_2{\cdot}3H_2O$ (11.3 mg in 500 μL of 9:1 $CDCl_3/CD_3OD$). A ^{1}H NMR spectrum recorded at 298 K showed the quantitative and instantaneous formation of $\mathbf{1}_{Cd}$·**PbOAc**.

Synthesis of an Analytical Sample of $\mathbf{1}_{Hg}$·PbOAc,TBA. Porphyrin **1** (30 mg, 0.024 mmol) was dissolved in $CHCl_3$ (5.4 mL), and then $AcO^-NBu_4^+$ (36 mg, 0.119 mmol), 300 μL (0.024 mmol, 1 equiv) of a stock solution of $Pb(OAc)_2{\cdot}3H_2O$ (36 mg in 1.2 mL of MeOH), and 300 μL (0.024 mmol, 1 equiv) of a stock solution of $Hg(OAc)_2$ (30 mg in 1.2 mL of MeOH), were successively added. A deep green color appeared instantaneously. The solution was stirred for 15 min at room temperature, and pentane (100 mL) was added. The solid was isolated by filtration, solubilized with a small amount of $CHCl_3$, and precipitated with pentane. This operation was repeated five times, leading to $\mathbf{1}_{Hg}$·**PbOAc,TBA** as a green solid (47 mg, quantitative). Anal. Calcd for $C_{98}H_{93}N_9O_{10}HgPb{\cdot}4H_2O$: C, 57.79; H, 5.00; N, 6.19. Found: C, 58.02; H, 4.62; N, 5.99. HRMS analysis (ESI-

dx.doi.org/10.1021/ja501926f | J. Am. Chem. Soc. 2014, 136, 6698−6715

TOF, negative-ion mode): calcd for $C_{82}H_{57}N_8O_{10}{}^{202}Hg^{208}Pb$ [M − TBA]$^-$ m/z 1723.3676, found m/z 1723.3669. ^{1}H NMR ($CDCl_3$, 298 K): δ 10.00 (s_b, 1H, NHCO), 9.26 (d, 1H, J = 5 Hz, $H_{\beta pyr}$), 9.22 (d, 1H, J = 8 Hz, HAr_{meso}), 9.15 (d, 1H, J = 5 Hz, $H_{\beta pyr}$), 9.13 (d, 1H, J = 8 Hz, HAr_{meso}), 9.08 (d, 1H, J = 8 Hz, HAr_{meso}), 9.07 (d, 1H, J = 5 Hz, $H_{\beta pyr}$), 9.04 (d, 1H, J = 5 Hz, $H_{\beta pyr}$), 8.99 (d, 1H, J = 5 Hz, $H_{\beta pyr}$), 8.96 (d, 1H, J = 8 Hz, HAr_{meso}), 8.88 (dd, 1H, J_1 = 1 Hz, J_2 = 8 Hz, HAr_{meso}), 8.83 (d, 1H, J = 5 Hz, $H_{\beta pyr}$), 8.74 (m, 2H, $H_{\beta pyr}$), 8.68 (s_b, 1H, NHCO), 8.35 (dd, 1H, J_1 = 1 Hz, J_2 = 7 Hz, HAr_{meso}), 8.21 (dd, 1H, J_1 = 1 Hz, J_2 = 7 Hz, HAr_{meso}), 8.10 (s, 1H, NHCO), 7.88 (dt, 1H, J_1 = 1 Hz, J_2 = 7 Hz, HAr_{meso}), 7.86 (dt, 1H, J_1 = 1 Hz, J_2 = 7 Hz, HAr_{meso}), 7.82 (d, 1H, J = 8 Hz, HAr_{meso}), 7.79 (t, 1H, J = 8 Hz, HAr_{meso}), 7.78 (dt, 1H, J_1 = 1 Hz, J_2 = 7 Hz, HAr_{meso}), 7.70 (s, 1H, NHCO), 7.63 (t, 1H, J = 8 Hz, HAr_{meso}), 7.62 (d, 1H, J = 7 Hz, HAr_{strap}), 7.58 (t, 1H, J = 7 Hz, HAr_{meso}), 7.49 (t, 1H, J = 8 Hz, HAr_{meso}), 7.48 (d, 1H, J = 7 Hz, HAr_{strap}), 7.46 (d, 1H, J = 7 Hz, HAr_{strap}), 7.39 (d, 1H, J = 7 Hz, HAr_{strap}), 7.37 (t, 1H, J = 7 Hz, HAr_{meso}), 7.01 (t, 1H, J = 7 Hz, HAr_{strap}), 6.92 (t, 1H, J = 7 Hz, HAr_{strap}), 6.91 (t, 1H, J = 7 Hz, HAr_{strap}), 6.87 (t, 1H, J = 7 Hz, HAr_{strap}), 6.82 (d, 1H, J = 7 Hz, HAr_{strap}), 6.79 (d, 1H, J = 7 Hz, HAr_{strap}), 6.73 (d, 1H, J = 7 Hz, HAr_{strap}), 6.61 (d, 1H, J = 7 Hz, HAr_{strap}), 5.92 (s, 1H, HAr_{strap}), 5.64 (s, 1H, HAr_{strap}), 5.44 (s, 1H, HAr_{strap}), 5.35 (s, 1H, HAr_{strap}), 2.53 (m, 1H, CH_{benz}), 2.50 (m, 8H, α-$CH_2{}^{TBA}$), 2.40 (d, 1H, J = 11 Hz, CH_{benz}), 2.32 (t, 1H, J = 12 Hz, CH_{benz}), 2.15 (t, 1H, J = 12 Hz, CH_{benz}), 2.01 (d, 1H, J = 11 Hz, CH_{benz}), 1.87 (d, 1H, J = 12 Hz, CH_{benz}), 1.40 (t, 1H, J = 12 Hz, CH_{benz}), 1.31 (m, 1H, CHCO), 1.29 (m, 1H, CH_{benz}), 1.12 (t, 1H, J = 12 Hz, CHCO), 1.06 (quint, 8H, J = 7 Hz, β-$CH_2{}^{TBA}$), 0.84 (sext, 8H, J = 7 Hz, γ-$CH_2{}^{TBA}$), 0.63 (t, 12H, J = 7 Hz, $CH_3{}^{TBA}$), 0.39 (s, 3H, CH_3COO).

Synthesis of an Analytical Sample of 1_{Cd}·PbOAc,TBA. The same protocol as that described above for the preparation of **1_{Hg}·PbOAc,TBA** was used, with 300 μL (0.023 mmol, 1 equiv) of a stock solution of $Cd(OAc)_2{\cdot}2H_2O$ (25 mg in 1.2 mL of MeOH), instead of the $Hg(OAc)_2$ methanolic solution. The complex **1_{Cd}·PbOAc,TBA** was isolated as a green solid in quantitative yield (45 mg). Anal. Calcd for $C_{98}H_{93}N_9O_{10}CdPb{\cdot}4H_2O$: C, 60.41; H, 5.22; N, 6.47. Found: C, 60.19; H, 4.80; N, 6.08. HRMS analysis (ESI-TOF, negative-ion mode): calcd for $C_{82}H_{57}N_8O_{10}{}^{114}Cd^{208}Pb$ [M − TBA]$^-$ m/z 1635.3003, found m/z 1635.3017. ^{1}H NMR ($CDCl_3$, 298 K): δ 9.48 (s, 1H, NHCO), 9.24 (d, 1H, J = 4 Hz, $H_{\beta pyr}$), 9.17 (d, 1H, J = 8 Hz, HAr_{meso}), 9.10 (d, 1H, J = 4 Hz, $H_{\beta pyr}$), 9.05 (d, 1H, J = 8 Hz, HAr_{meso}), 9.02 (d, 1H, J = 4 Hz, $H_{\beta pyr}$), 9.00 (d, 1H, J = 8 Hz, HAr_{meso}), 8.98 (d, 1H, J = 8 Hz, HAr_{meso}), 8.97 (s, 1H, NHCO), 8.95 (d, 1H, J = 4 Hz, $H_{\beta pyr}$), 8.86 (d, 1H, J = 4 Hz, $H_{\beta pyr}$), 8.79 (d, 1H, J = 4 Hz, $H_{\beta pyr}$), 8.76 (d, 1H, J = 8 Hz, HAr_{meso}), 8.64 (s_b, 2H, $H_{\beta pyr}$), 8.36 (dd, 1H, J_1 = 1 Hz, J_2 = 7 Hz, HAr_{meso}), 8.18 (dd, 1H, J_1 = 1 Hz, J_2 = 7 Hz, HAr_{meso}), 8.00 (s, 1H, NHCO), 7.88 (d, 1H, J = 8 Hz, HAr_{meso}), 7.86 (t, 1H, J = 7 Hz, HAr_{meso}), 7.84 (t, 1H, J = 7 Hz, HAr_{meso}), 7.79 (t, 1H, J = 7 Hz, HAr_{meso}), 7.76 (s, 1H, NHCO), 7.74 (t, 1H, J = 7 Hz, HAr_{meso}), 7.60 (t, 1H, J = 7 Hz, HAr_{meso}), 7.59 (d, 1H, J = 8 Hz, HAr_{strap}), 7.57 (t, 1H, J = 7 Hz, HAr_{meso}), 7.48 (d, 1H, J = 8 Hz, HAr_{strap}), 7.45 (t, 1H, J = 7 Hz, HAr_{meso}), 7.41 (d, 1H, J = 8 Hz, HAr_{strap}), 7.40, (t, 1H, J = 7 Hz, HAr_{meso}), 7.39 (d, 1H, J = 8 Hz, HAr_{strap}), 6.97 (t, 1H, J = 7 Hz, HAr_{meso}), 6.92 (t, 1H, J = 7 Hz, HAr_{meso}), 6.90 (t, 1H, J = 7 Hz, HAr_{meso}), 6.88 (t, 1H, J = 7 Hz, HAr_{meso}), 6.80 (d, 2H, J = 7 Hz, HAr_{meso}), 6.65 (d, 1H, J = 7 Hz, HAr_{meso}), 6.59 (d, 1H, J = 7 Hz, HAr_{meso}), 5.79 (s, 1H, HAr_{strap}), 5.63 (s, 1H, HAr_{strap}), 5.49 (s, 1H, HAr_{strap}), 5.45 (s, 1H, HAr_{strap}), 2.77 (m, 8H, α-$CH_2{}^{TBA}$), 2.44 (d, 1H, J = 12 Hz, CH_{benz}), 2.42 (d, 1H, J = 12 Hz, CH_{benz}), 2.07 (t, 1H, J = 12 Hz, CH_{benz}), 2.01 (t, 1H, J = 12 Hz, CH_{benz}), 1.79 (d, 1H, J = 12 Hz, CH_{benz}), 1.73 (d, 1H, J = 12 Hz, CH_{benz}), 1.48 (t, 1H, J = 12 Hz, CH_{benz}), 1.37 (t, 1H, J = 12 Hz, CH_{benz}), 1.32 (m, 1H, CHCO), 1.29 (m, 8H, β-$CH_2{}^{TBA}$), 1.06 (sext, 8H, J = 7 Hz, γ-$CH_2{}^{TBA}$), 0.89 (m, 1H, CHCO), 0.76 (t, 12H, J = 7 Hz, $CH_3{}^{TBA}$), 0.48 (s, 3H, CH_3COO).

Crystal Data for Complex 1HgPb. $C_{86}H_{72}HgN_8O_{11}PbS_3{\cdot}CH_4O{\cdot}2(CH_2Cl_2)$; M = 2099.37. APEXII, Bruker-AXS diffractometer, Mo Kα radiation (λ = 0.710 73 Å), T = 150(2) K; triclinic $P\bar{1}$, a = 12.5099(4) Å, b = 13.1210(5) Å, c = 26.2852(8) Å, α = 80.2710(10)°, β = 81.9170(10)°, γ = 88.1610(10)°, V = 4210.1(2) Å^3, Z = 2, d = 1.656 g.cm^{-3}, μ = 4.087 mm^{-1}. The structure was solved by direct methods using the SIR97 program[37] and then refined with full-matrix least-squares methods based on F2 (SHELXL-97)[38] with the aid of the WINGX[39] program. All non-hydrogen atoms were refined with anisotropic atomic displacement parameters. H atoms were finally included in their calculated positions. A final refinement on F2 with 18 950 unique intensities and 1029 parameters converged at ωR(F2) = 0.1332 ($R(F)$ = 0.0594) for 16 267 observed reflections with $I > 2\sigma(I)$; CCDC 987556.

Crystal Data for Complex 1CdPb. $C_{86}H_{72}CdN_8O_{11}PbS_3{\cdot}C_{85}H_{70}CdN_8O_{11}PbS_2$; M = 3572.49. APEXII, Bruker-AXS diffractometer, Mo Kα radiation (λ = 0.710 73 Å), T = 150(2) K; monoclinic $P2_1$, a = 12.7300(12) Å, b = 49.192(4) Å, c = 13.2149(12) Å, β = 92.641(2)°, V = 8266.6(13) Å^3, Z = 2, d = 1.435 g.cm^{-3}, μ = 2.417 mm^{-1}. The structure was solved by direct methods using the SIR97 program[37] and then refined with full-matrix least-squares methods based on F2 (SHELXL-97)[38] with the aid of the WINGX[39] program. The contribution of the disordered solvents to the calculated structure factors was estimated following the BYPASS algorithm,[40] implemented as the SQUEEZE option in PLATON.[41] A new data set, free of solvent contribution, was then used in the final refinement. All non-hydrogen atoms were refined with anisotropic atomic displacement parameters. H atoms were finally included in their calculated positions. A final refinement on F2 with 33 903 unique intensities and 1509 parameters converged at ωR(F2) = 0.1742 ($R(F)$ = 0.0718) for 28 053 observed reflections with $I > 2\sigma(I)$; CCDC 987555.

■ ASSOCIATED CONTENT

Ⓢ Supporting Information

^{1}H NMR titration studies of **1** with Hg(II) and Cd(II); ^{13}C NMR spectra, 2D COSY, HMQC, ROESY NMR spectra, and variable temperature ^{1}H NMR spectra of **1_{Hg}·PbOAc,TBA** and **1_{Cd}·PbOAc,TBA**; 2D ROESY spectra and variable temperature ^{1}H NMR spectra of **1_{Hg}·PbOAc** and **1_{Cd}·PbOAc**; ^{1}H NMR studies of the influence of DMAP on Hg(II) complexes of **1**; estimation of the activation barriers for the first and second dynamic processes displayed by **1_{Cd}·PbOAc**; temperature dependence of the ^{207}Pb chemical shifts (δ) of **1_{Bi}·PbOAc**, **1_{Pb}·PbOAc**, and **1_{Cd}·PbOAc**; additional comments concerning the X-ray structure of **1CdPb**. This material is available free of charge via the Internet at http://pubs.acs.org.

■ AUTHOR INFORMATION

Corresponding Author

stephane.legac@univ-rennes1.fr; bernard.boitrel@univ-rennes1.fr

Notes

The authors declare no competing financial interest.

■ ACKNOWLEDGMENTS

We are grateful to ANR (research program ANR BLANC "BIBI-CHEMAP", ANR-12-B507-0006-01) and "La Ligue Contre Le Cancer" for financial support. L.F. thanks Prof. Michel Luhmer (Université Libre de Bruxelles, ULB) for stimulating discussions and the access to the NMR facilities and the "Fonds de la Recherche Scientifique" (F.R.S.-FNRS) and ULB for financial support.

■ REFERENCES

(1) (a) Lehn, J.-M. *Science* **2002**, *295*, 2400−2403. (b) Lehn, J.-M. *Angew. Chem., Int. Ed.* **2013**, *52*, 2836−2850.

(2) (a) Lehn, J.-M. *Chem.—Eur. J.* **1999**, *5*, 2455−2463. (b) Rowan, S. J.; Cantrill, S. J.; Cousins, G. R. L.; Sanders, J. K. M.; Stoddart, J. F. *Angew. Chem., Int. Ed.* **2002**, *41*, 898−952. (c) Corbett, P. T.; Leclaire,

J.; Vial, L.; West, K. R.; Wietor, J.-L.; Sanders, J. K. M.; Otto, S. *Chem. Rev.* **2006**, *106*, 3652−3711.
(3) (a) Giuseppone, N. *Acc. Chem. Res.* **2012**, *45*, 2178−2188. (b) Moulin, E.; Cormos, G.; Giuseppone, N. *Chem. Soc. Rev.* **2012**, *41*, 1031−1049.
(4) Beletskaya, I.; Tyurin, V. S.; Tsivadze, A. Y.; Guilard, R.; Stern, C. *Chem. Rev.* **2009**, *109*, 1659−1713.
(5) (a) Stulz, E.; Ng, Y.-F.; Scott, S. M.; Sanders, J. K. M. *Chem. Commun.* **2002**, 524−525. (b) Stulz, E.; Scott, S. M.; Bond, A. D.; Teat, S. J.; Sanders, J. K. M. *Chem.—Eur. J.* **2003**, *9*, 6039−6048. For dynamic libraries of metalloporphyrins based on thiol-disulfide exchange, see: (c) Kieran, A. L.; Bond, A. D.; Belenguer, A. M.; Sanders, J. K. M. *Chem. Commun.* **2003**, 2674−2675. (d) Kieran, A. L.; Pascu, S. I.; Jarrosson, T.; Sanders, J. K. M. *Chem. Commun.* **2005**, 1276−1278. (e) Kieran, A. L.; Pacsu, S. I.; Jarrosson, T.; Gunter, M. J.; Sanders, J. K. M. *Chem. Commun.* **2005**, 1842−1844.
(6) Kondratuk, D. V.; Perdigao, L. M. A.; O'Sullivan, M. C.; Svatek, S.; Smith, G.; O'Shea, J. N.; Beton, P. H.; Anderson, H. L. *Angew. Chem., Int. Ed.* **2012**, *51*, 6696−6699.
(7) Pawlicki, M.; Latos-Grażyacński, L. *Angew. Chem., Int. Ed.* **2012**, *51*, 11205−11207.
(8) For a review dealing with transmetallation processes in self-assembled supramolecular complexes, see: Carnes, M. E.; Collins, M. S.; Johnson, D. W. *Chem. Soc. Rev.* **2014**, *43*, 1825−1834.
(9) (a) Halime, Z.; Lachkar, M.; Roisnel, T.; Furet, E.; Halet, J.-F.; Boitrel, B. *Angew. Chem., Int. Ed.* **2007**, *46*, 5120−5124. (b) Motreff, N.; Le Gac, S.; Luhmer, M.; Furet, E.; Halet, J.-F.; Roisnel, T.; Boitrel, B. *Angew. Chem., Int. Ed.* **2011**, *50*, 1560−1564. (c) Le Gac, S.; Najjari, B.; Motreff, N.; Remaud-Le Saec, P.; Faivre-Chauvet, A.; Dimanche-Boitrel, M.-T.; Morgenstern, A.; Bruchertseifer, F.; Lachkar, M.; Boitrel, B. *Chem. Commun.* **2011**, *47*, 8554−8556. (d) Najjari, B.; Le Gac, S.; Roisnel, T.; Dorcet, V.; Boitrel, B. *J. Am. Chem. Soc.* **2012**, *134*, 16017−16032. (e) Le Gac, S.; Najjari, B.; Dorcet, V.; Roisnel, T.; Fusaro, L.; Luhmer, M.; Furet, E.; Halet, J.-F.; Boitrel, B. *Chem.—Eur. J.* **2013**, *19*, 11021−11038. (f) Le Gac, S.; Fusaro, L.; Dorcet, V.; Boitrel, B. *Chem.—Eur. J.* **2013**, *19*, 13376−13386. (i) Newton's cradle is a device used to illustrate conservation of momentum and energy. It consists of a series of equal pendulums in a row, and a swinging motion is induced by the release of a sphere pulled away at one extremity. Collision with a second sphere sends the momentum through the series of spheres, causing the opposite swinging motion of a sphere at the other extremity of the device. Swinging back and collision with the series of resting spheres leads to the reverse swinging motion of the first sphere.
(10) For earlier work, see: Le Gac, S.; Boitrel, B. *J. Porphyrins Phthalocyanines* **2012**, *16*, 537−544 and references therein.
(11) Such bimetallic complexes involving a regular porphyrin as bridging ligand have been scarcely reported: (a) Tsutsui, M.; Hrung, C. P.; Ostfeld, D.; Srivastava, T. S.; Cullen, D. L.; Meyer, E. F., Jr. *J. Am. Chem. Soc.* **1975**, *97*, 3952−3965. (b) Mashiko, T.; Reed, C. A.; Haller, K. J.; Scheidt, W. R. *Inorg. Chem.* **1984**, *23*, 3192−3196. (c) Ciurli, S.; Gambarotta, S.; Floriani, C.; Chiesi-Villa, A.; Guasfini, C. *Angew. Chem., Int. Ed. Engl.* **1986**, *25*, 553−554. (d) Arnold, J.; Dawson, D. Y.; Hoffman, C. C. *J. Am. Chem. Soc.* **1993**, *115*, 2707−2713. (e) Lai, J.-J.; Khademi, S.; Meyer, E. F., Jr.; Cullen, D. L.; Smith, K. M. *J. Porphyrins Phthalocyanines* **2001**, *5*, 621−627.
(12) For a detailed description of the hanging-atop coordination mode with Pb(II), see: Le Gac, S.; Najjari, B.; Fusaro, L.; Roisnel, T.; Dorcet, V.; Luhmer, M.; Furet, E.; Halet, J.-F.; Boitrel, B. *Chem. Commun.* **2012**, *48*, 3724−3726.
(13) The notation $\mathbf{1}_{\mathbf{M}}$ or $\mathbf{1}^{\mathbf{M}}$ refers to the location of a metal ion, bound out-of-plane to the N-core, on one or the other side of the macrocycle. For instance, $\mathbf{1}_{\mathbf{Bi}}$**·PbOAc** (with Bi subscripted) corresponds to an out-of-plane Bi(III) cation arbitrarily represented bound to the lower side of the porphyrin, as drawn in Figure 1.
(14) In the HAT coordination, the distance of a metal ion to the porphyrin mean plane is ca. 1 Å longer than in the OOP coordination, as observed in X-ray structures with Pb(II) and Bi(III). Therefore, a magnitude of ca. 1 Å is expected for the intraligand motion of a cation. See refs 9d and 12.
(15) Double translocation processes have been scarcely reported: (a) Fabbrizzi, L.; Foti, F.; Patroni, S.; Pallavicini, P.; Taglietti, A. *Angew. Chem., Int. Ed.* **2004**, *43*, 5073−5077. (b) Aurora, M.; Boiocchi, M.; Dacarro, G.; Foti, F.; Mangano, C.; Pallavicini, P.; Patroni, S.; Taglietti, A.; Zanoni, R. *Chem.—Eur. J.* **2006**, *12*, 5535−5546. (c) Colasson, B.; Le Poul, N.; Le Mest, Y.; Reinaud, O. *J. Am. Chem. Soc.* **2010**, *132*, 4393−4398.
(16) The unusual fast kinetics of metalation of **1** results from a deconvolution of the metal salt by the overhanging COO^- group, facilitating the formation of an intermediate sitting-atop complex; see ref 12. For a reference dealing with deconvolution processes, see: (a) Buchler, J. W. In *Porphyrins and Metalloporphyrins*; Smith, K. M., Ed.; Elsevier: Amsterdam, 1975; pp 157. For an early example of assisted metallation of a porphyrin chelate appended with carboxylate groups, see: (b) Buckingham, D. A.; Clark, C. R.; Webley, W. S. *J. Chem. Soc., Chem. Commun.* **1981**, 192−194.
(17) Transmetalation processes with porphyrins have been studied with the aim of increasing the rate of insertion of a metal ion. A general mechanism involves the distortion of the porphyrin macrocycle induced by a large metal ion as a means to lower the free activation energy for the insertion of a smaller cation. The release of the first large metal ion, to the best of our knowledge, has not been exploited so far. Selected references: (a) Tabata, M.; Miyata, W.; Nahar, N. *Inorg. Chem.* **1995**, *34*, 6492−6496. (b) Grant, C., Jr.; Hambright, P. *J. Am. Chem. Soc.* **1969**, *91*, 4195−4198.
(18) Identification of the known monometallic and homobimetallic species of **1** was achieved by careful comparison of the data with their NMR patterns recorded under the same experimental conditions.
(19) No trace of monometallic complexes was observed. Only a trace of $\mathbf{1}_{\mathbf{Pb}}$**·PbOAc** was observed in the Hg(II)/Pb(II) experiment.
(20) At 223 K, δ_{CH_3COO} = +0.24 and −0.23 ppm for $\mathbf{1}_{\mathbf{Pb}}$**·PbOAc** and $\mathbf{1}_{\mathbf{Cd}}$**·CdOAc**, respectively; see refs 9d and 9f. The presence of a HAT CdOAc is thus excluded.
(21) We hypothesize that the stereochemically active lone pair of lead, responsible for a strongly hemidirected coordination sphere, is at the origin of a higher complementarity of the PbOAc moiety with the HAT binding site, allowing a stronger second sphere of coordination with the CONH group of the straps (H-bonding interaction).
(22) It is noteworthy that these conditions are opposite of those optimized with a related compound bearing overhanging carboxylic acid and amide groups on opposite sides (compound **3**, Figure 1, top right). Indeed, the N-core-bound Cd(II) binds preferentially to the carbonyl of the COO^- vs the CONH group, which weakens the complexation of the HAT Pb(II). The absence of a base led to the opposite stereoselectivity [Cd(II) binds preferentially to the carbonyl of the CONH vs the COOH group] and to a higher affinity of the HAT Pb(II); see ref 9e.
(23) A Pb(II) monometallic complex of **1** has never been observed.
(24) Wrackmeyer, B.; Contreras, R. *Annu. Rep. NMR Spectrosc.* **1992**, *24*, 267−329.
(25) Summers, M. F. *Coord. Chem. Rev.* **1988**, *86*, 43−134.
(26) Wrackmeyer, B.; Horchler, K. *Annu. Rep. NMR Spectrosc.* **1990**, *22*, 249−306.
(27) The assignment of the HAT and OOP signals in $\mathbf{1}_{\mathbf{Pb}}$**·PbOAc** was done by comparison with $\mathbf{1}_{\mathbf{Bi}}$**·PbOAc**; see the SI.
(28) In contrast to Cd and Pb, Hg and Pb cannot be differentiated on the basis of the relative intensity of the diffraction peaks because of their close electron density. They have been assigned on the basis of the comparison of their displacement from the mean plane with the metal atoms in **1CdPb**. Indeed, one of the metal atoms in **1HgPb** presents a large OOP displacement very similar to that of Pb in **1CdPb** (∼1.86 Å; see the text).
(29) Two molecules are present in the crystal lattice of **1CdPb** (only one of them is described herein). They differ by the solvent molecules weakly bound to Cd (methanol or dimethyl sulfoxide).
(30) For the major diastereoisomer, the binding of the PbOAc moiety to the left side of the strap as drawn in Scheme 1 is based on

several X-ray structures of related bimetallic complexes; see refs 9d and 9e.
(31) No effect of the addition of DMAP on the ^{1}H NMR pattern of $\mathbf{1}_{Pb}$·**PbOAc** was observed.
(32) All of these complexes tolerate a large amount of AcO^{-} (ca. 40 equiv). Therefore, the reverse formation of $\mathbf{1}_{Hg}$·**PbOAc** is not due to a lack of stability of one of the homobimetallic complexes.
(33) (a) Kozminski, W.; Jackowski, K. *Magn. Reson. Chem.* **2000**, *38*, 459−462. (b) Schraml, J.; Sandor, P.; Korec, S.; Krump, M.; Foller, B. *Magn. Reson. Chem.* **2013**, *51*, 403−406.
(34) Kennedy, M. A.; Sessler, J. L.; Murai, T.; Ellis, P. *Inorg. Chem.* **1990**, *29*, 1050−1054.
(35) Berra, A.; Di Vona, M. L.; Floris, B.; Licoccia, S. *Appl. Organometal. Chem.* **2000**, *14*, 565−569.
(36) Claudio, E. S.; Horts, M. A.; Forde, C. E.; Stern, C. L.; Zart, M. K.; Godwin, H. A. *Inorg. Chem.* **2000**, *39*, 1391−1397.
(37) Altomare, A.; Burla, M. C.; Camalli, M.; Cascarano, G.; Giacovazzo, C.; Guagliardi, A.; Moliterni, A. G. G.; Polidori, G.; Spagna, R. *J. Appl. Crystallogr.* **1999**, *32*, 115−119.
(38) Sheldrick, G. M. *Acta Crystallogr., Sect. A* **2008**, *A64*, 112−122.
(39) Farrugia, L. J. *J. Appl. Crystallogr.* **1999**, *32*, 837−838.
(40) Van der Sluis, P.; Spek, A. L. *Acta Crystallogr., Sect. A* **1990**, *46*, 194−201.
(41) Spek, A. L. *J. Appl. Crystallogr.* **2003**, *36*, 7−13.